Introducing Rhetorical Parallelism Detection:
A New Task with Datasets, Metrics, and Baselines

Stephen Bothwell
University of Notre Dame
sbothwel@nd.edu

Justin DeBenedetto
Villanova University
justin.debenedetto@villanova.edu

Theresa Crnkovich　　**Hildegund Müller**　　**David Chiang**
University of Notre Dame
{tcrnkovi,hmuller,dchiang}@nd.edu

Abstract

Rhetoric, both spoken and written, involves not only content but also style. One common stylistic tool is *parallelism*: the juxtaposition of phrases which have the same sequence of linguistic (*e.g.*, phonological, syntactic, semantic) features. Despite the ubiquity of parallelism, the field of natural language processing has seldom investigated it, missing a chance to better understand the nature of the structure, meaning, and intent that humans convey. To address this, we introduce the task of *rhetorical parallelism detection*. We construct a formal definition of it; we provide one new Latin dataset and one adapted Chinese dataset for it; we establish a family of metrics to evaluate performance on it; and, lastly, we create baseline systems and novel sequence labeling schemes to capture it. On our strictest metric, we attain F_1 scores of 0.40 and 0.43 on our Latin and Chinese datasets, respectively.

1 Introduction

Ueni, uidi, uici,[1] or, "I came, I saw, I conquered" – why is this saying so memorable? One reason is the high degree of *parallelism* it exhibits in its morphology (each verb is first-person, singular, perfect tense), phonology (each verb starts with /w/ and ends with /iː/), and prosody (each verb has two long syllables with accent on the first). In similar sayings (as in Fig. 1), syntax and semantics also contribute. The related elements generally occur in either the same order or in an inverted order.

Parallelism is organically employed in many argumentative structures (*e.g.*, "on the one hand . . . on the other hand . . ."), making parallelism a routine rhetorical figure. The rhetorical impact of

---

[1] Popularly attributed to Julius Caesar (Suetonius Tranquillus, 1993). In Classical Latin, *u* and *v* were graphical variants of one letter; as a consonant, it was pronounced /w/. Following common practice, we write it as *u*. We also write *i* and *j* as *i*.
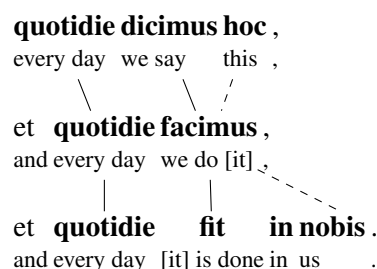

Figure 1: Example three-way parallelism from Augustine's *Sermones* (Sermon 181, Section 8). Solid lines connect words with multiple linguistic features in common; dashed lines indicate a weaker connection.

these structures is apparent even for audiences not schooled in classical rhetoric. Recognition of parallelism, then, is important for grasping the structure, meaning, and intent that humans wish to convey; thus, the computational modeling of parallelism is both an interesting and practical problem.

However, because parallelism can occur at so many levels linguistically—often with no lexical overlap—modeling parallelism computationally is difficult. As a first foray into studying the problem of rhetorical parallelism detection (RPD) and enabling others to study it, we present in this paper multiple public datasets, metrics, and models for it.

For one dataset, we turn to the Latin sermons of Augustine of Hippo (354–430). Augustine had been trained as a rhetorician and had taught the craft of secular rhetoric before his conversion to Christianity. However, upon becoming a preacher, he consciously replaced the adorned style of late ancient rhetoric with a style streamlined toward speaking well with diverse North African congregations. Parallelism frequently marked this style.

Augustine did not just employ parallelism stylistically, however; he also theorized about it. In his work *De Doctrina Christiana*, Augustine described three rhetorical styles, or *genera dicendi* ("ways of

speaking") (Augustine of Hippo, 1995); from these, he characterized the *genus temperatum* ("moderate style") by highly-parallel passages.[2] Thus, his sermons are ideal for studying parallelism. In addition, his theory implies that parallelism detection may be useful for automatic stylistic analysis. Already, it has been used to analyze discourse structure (Guégan and Hernandez, 2006), summarize documents (Alliheedi, 2012), identify idioms (Adewumi et al., 2022), evaluate student writing (Song et al., 2016), study political speech (Tan et al., 2018) and detect fake news (Gautam and Jerripothula, 2020).

Parallelism detection may also have broader NLP applications. In syntactic parsing, in the sentence *I saw a man with a mustache and a woman with a telescope*, the reading where *telescope* modifies *saw* is all but ruled out because it would violate parallelism. Thus, modeling parallelism could assist in syntactic disambiguation. Parallelism is also vital in disfluency detection, as speakers tend to maintain prior syntactic context when amending verbal errors (Zayats and Ostendorf, 2019).

Toward such ends, we establish the task of rhetorical parallelism detection (RPD, Section 2). We create one dataset from Augustine's sermons and adapt another consisting of Chinese student essays (Section 4), establish evaluation metrics (Section 5), and investigate baseline models (Section 6). By automatically learning and exploiting relationships among linguistic features, we achieve roughly a 40% F_1 score on both datasets' test sets (Section 7).

2 Task Definition

Moving away from the sentence-level conceptions of Guégan and Hernandez (2006) and Song et al. (2016), we formalize the task of **rhetorical parallelism detection** (RPD). Broadly, we deem sequences to be *parallel* if they meet two conditions:

1. **Locality**: Parallel structures should be within temporal proximity of one another for two related reasons. First, structures that are close by are more likely to be intentional rather than incidental in the mind of the speaker/author. Second, for parallel structures to be rhetorically effective, they must be consecutive enough to be recalled by the listener/reader.

2. **Linguistic Correspondence**: Parallel structures should have some linguistic features in common, which could include features of

phonology, morphology, syntax, semantics, or even *style*. The features could be the same (*e.g.*, the repeated sounds in *ueni, uidi, uici*) or diametrically opposed (*e.g.*, the opposite meanings in *a time to be born and a time to die*). These features typically occur in the same order or the opposite order.

Suppose that we have a document **w**, which is a sequence of tokens $w_1 \ldots w_n$. A **span** of **w** is a pair (i, j), where $1 \leq i \leq j \leq n$, whose **contents** are the tokens $w_i \ldots w_j$. We say that two spans (i_1, j_1) and (i_2, j_2) are **overlapping** if they have at least one token in common—that is, $i_1 \leq i_2 \leq j_1$ or $i_2 \leq i_1 \leq j_2$. Meanwhile, they are **nested** if $i_1 \leq i_2 \leq j_2 \leq j_1$ or $i_2 \leq i_1 \leq j_1 \leq j_2$.

A **parallelism** is a set of two or more non-overlapping spans whose contents are parallel. We call these spans the **branches** of a parallelism. An example of a complete parallelism with three branches is given in Fig. 1. RPD, then, is the task of identifying all of the parallelisms in a text.

Let *P* be a set of parallelisms. Then *P* falls into one of three categories:

1. *P* is **flat** if all the branches of every parallelism in *P* are pairwise non-overlapping.

2. *P* is **nested** if some pair of its branches nest and no pair of its branches overlap without also being nested.

3. *P* is **overlapping** if it contains some pair of branches which overlap.

Our Augustinian Sermon Parallelism (ASP) dataset (see Section 4) is nested, and the Paibi Student Essay (PSE) dataset (Song et al., 2016) is flat.[3] Although our baseline models only predict flat sets of parallelisms, our evaluations include nested ones.

3 Related Work

In this section, we connect two subareas of NLP to RPD in order to display their relation to and influence on its development.

3.1 Automated writing evaluation

Arguably, the main research area that has explored RPD is automated writing evaluation (AWE). Since its inception (Page, 1966), AWE has aimed to reduce instructor burden by swiftly scoring essays;

---

[2] See chapters 4.20.40; 20.44; 21.47f.

[3] Song et al.'s dataset was not originally named but has been given a name through its inclusion in this work.

Dataset	Documents	Sections	Tokens	Branched Tokens	Branches	Parallelisms
ASP	80	477	134, 956	19, 701	4, 651 (39)	2, 062 (14)
PSE-I	409	3, 855	241, 203	25, 529	2, 153 (0)	786 (0)

Table 1: Dataset frequency statistics for both of the datasets featured in this paper. "Sections" are defined as natural partitions of documents, such as divisions determined by editors (ASP) or natural paragraphs (PSE-I). "Branched Tokens" refer to all tokens involved in a branch. Parenthesized values refer to the nested subset of a given quantity.

Dataset	Parallelisms per Section	Branches per Parallelism	Branch Distance (Tokens)	Branch Size (Tokens)	NLO (Branches)	% Pairs with No LO
ASP	4.32 ± 3.22	2.26 ± 0.68	2.54 ± 2.29	4.24 ± 2.72	0.24 ± 0.19	24.17%
PSE-I	1.92 ± 1.47	2.74 ± 0.75	2.41 ± 4.00	11.86 ± 7.09	0.31 ± 0.15	2.30%

Table 2: Dataset derived statistics. All figures but the last one are means with standard deviations. The lexical overlap (LO) metrics are normalized with respect to the union of branches' token multisets.

however, especially with the involvement of neural networks, it seems to be limited in its pedagogical benefit because of its inability to give sufficient feedback (Ke and Ng, 2019; Beigman Klebanov and Madnani, 2020).

Concerning RPD, Song *et al.* explored parallel structure as a critical rhetorical device for evaluating writing quality (Song et al., 2016). Construing parallelism detection as a sentence pair classification problem, they achieved 72% F_1 for getting entire parallelisms correct on their dataset built from Chinese mock exam essays via a random forest classifier with hand-engineered features. Subsequent work used RNNs (Dai et al., 2018) and CNNs with some custom features (Liu et al., 2022). Such work has also been applied in the IFlyEA assessment system to provide students with stylistic feedback (Gong et al., 2021).

Compared to that work, our formalization of RPD permits a token-level (as opposed to sentence-level) granularity for parallel structure. In line with this, we approach RPD in terms of sequence labeling instead of classification. Moreover, we provide the first (to our knowledge) public release of token-level parallelism detection data (see Section 4).

3.2 Disfluency detection

RPD closely resembles and is notably inspired by disfluency detection (DD). DD's objective is generally to detect three components of a speech error: the *reparandum* (the speech to be replaced), the *interregnum* (optional intervening speech), and the *repair* (optional replacing speech) (Shriberg, 1994). Because the *reparandum* and *repair* often relate in their syntactic and semantic roles, they (as with parallelisms) share many linguistic features.

DD has frequently been framed as a sequence labeling task. Some previous models use schemes which adapt BIO tagging (Georgila, 2009; Ostendorf and Hahn, 2013; Zayats et al., 2014, 2016), while others (Hough and Schlangen, 2015) have proposed novel tagging schemes on the basis of prior theory (Shriberg, 1994) and the Switchboard corpus's notation (Meteer and Taylor, 1995), augmenting tags with numerical links to indicate relationships between reparanda and repairs.

We employ elements of both types of tagging schemes: we directly adapt BIO tags to parallelisms, and, like Hough and Schlangen (2015), we also augment tags with numerical links to indicate relationships between branches (see Section 6.1).

4 Datasets

This paper presents two datasets for RPD: the Augustinian Sermon Parallelism (ASP) and Paibi Student Essay (PSE) datasets. We first describe steps taken for the individual datasets in Sections 4.1 and 4.2 before discussing shared preprocessing steps and data analyses in Sections 4.3 and 4.4.

4.1 Augustinian Sermon Parallelism Dataset

The ASP dataset consists of 80 sermons from the corpus of Augustine of Hippo (Augustine of Hippo, 2000a,b).[4] Our fourth author, an expert classicist and Augustine scholar, labeled these sermons for parallel structure using our annotation scheme. This scheme involves labeling branches and linking them to form parallelisms. We further distinguish between synchystic (same order) and chiastic (in-

---

[4]The ASP dataset is freely available at `https://github.com/Mythologos/Augustinian-Sermon-Parallelisms`.

(a) *ut   ipse* [*panis   esuriret*   ]₁ , [*satietas   sitiret*   ]₁ , [*uirtus*
so.that itself bread:NOM;SG hunger:IPFV;SBJV;3SG   ,   satiety:NOM;SG thirst:IPFV;SBJV;3SG   ,   strength:NOM;SG
infirmaretur   ]₁ , [*sanitas   uulneraretur*   ]₁ , [*uita   moraretur*   ]₁ ?
weaken:IPFV;SBJV;3SG   ,   health:NOM;SG wound:IPFV;SBJV;3SG   ,   life:NOM;SG die:IPFV;SBJV;3SG   ?
"... so that bread itself might hunger, satiety might thirst, strength might be weakened, health might be wounded, life might die?"

(b) [小草   更   绿   ]₁ , [天空   更   蓝   ]₁ , [生活   更   美好   ]₁ .
xiǎocǎo gèng lǜ   ,   tiānkōng gèng lán   ,   shēnghuó gèng měihǎo   .
grass   more green   ,   sky   more blue   ,   life   more good   .
"The grass is greener, the sky is bluer, and life is better."

Figure 2: Examples from the ASP and PSE datasets. Blue square brackets demarcate each branch, and numbering indicates the parallelism to which each branch belongs. We provide a word-by-word English translation, gloss some morphological features in branches, and present an idiomatic translation. Example (a) is from Sermon 207, Section 1. Example (b) is from Essay 1, Paragraph 5. For more ASP dataset examples, see Figs. 7 and 8.

verted order) parallelisms.[5] For more details on our annotation scheme, see Appendix A; for details on a verification of the dataset's quality through an inter-annotator agreement study, see Appendix C.

An example of Augustine's use of parallelism is presented in Fig. 2(a). In this subordinate clause, Augustine builds up a five-way parallelism. This parallelism not only boasts shared morphology and syntax through a series of subject-verb clauses, but it also presents *stylistic* parallelism. Each clause uses the rhetorical device of personification, presenting an object or abstract idea as an agent, and this device is paralleled to emphasize it. As this example shows, Augustine frequently layers linguistic features to compose parallelisms.

To preprocess the ASP data, we remove all capitalization, following previous work on Latin word embeddings (Bamman and Burns, 2020; Burns et al., 2021). We also employ the `LatinWordTokenizer` from the CLTK library to tokenize our data (Johnson et al., 2021).

4.2 Paibi Student Essay Dataset

The PSE dataset was created by Song et al. (2016) to improve automatic essay evaluation.[6] They collected a set of mock exam essays from Chinese senior high school students. Two annotators then marked parallel structure in these essays. Annotators labeled parallelism on the *sentence* rather than *span* level. On this task, they achieved an inter-annotator agreement of 0.71 according to the κ statistic (Carletta, 1996) over a set of 30 essays.

In Chinese, a 排比 (*pǎibǐ*, parallelism) is some-

times defined as having at least three branches (although the PSE dataset has many examples of two-branch parallelisms). One such three-way parallelism is given in Fig. 2(b), where both lexical repetition of the comparative adverb 更 (*gèng*) and syntactic parallelism help the sentence's three clauses to convey its message in a spirited manner.

We obtained 409 of the original 544 essays from the authors. The essays are annotated for inter-paragraph parallelisms, intra-paragraph parallelisms, and intra-sentence parallelisms. To adapt them for our use, we first excluded inter-paragraph parallelisms, as these do not satisfy our criterion of locality. Then, for each intra-sentence parallelism that had been annotated, our annotators marked the locations of the parallel branches. For more details about this annotation process, see Appendix A. We call this version of the dataset PSE-I, or the version only having parallelisms *inside* paragraphs. We retained the tokenization generated by the Language Technology Platform (LTP) (Che et al., 2010).

4.3 Data collection and preprocessing

Both datasets had annotations collected for them via the BRAT annotation tool (Stenetorp et al., 2012). In applying the parallelism annotations to the data, both datasets excluded punctuation from parallelisms. This was done to reduce annotator noise brought about by the inconsistent membership of punctuation in parallelisms.

After preprocessing each dataset, we split both into training, validation, optimization, and test sets. To do so, we attempted to keep the ratio of tokens inside parallelisms to tokens outside parallelisms as even as possible across each set, assuring that the sets were distributed similarly. For more details on our data splitting, see Appendix E.

---

[5]The terms *synchystic* and *chiastic* are used by analogy with the traditional rhetorical terms *synchysis* and *chiasmus*.

[6]The PSE dataset and its PSE-I variant are freely available at https://github.com/Mythologos/Paibi-Student-Essays.
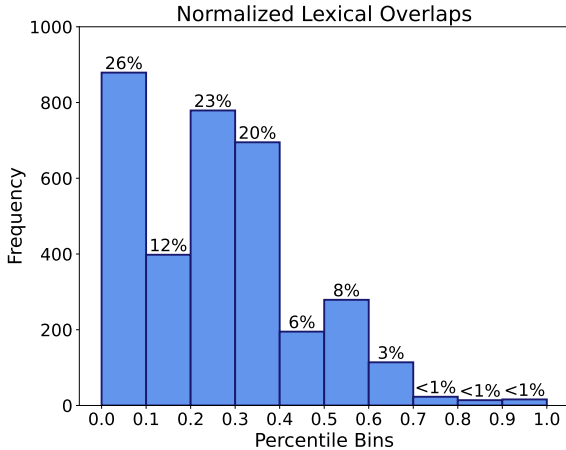
Figure 3: Histogram of normalized lexical overlap for all paired branches in the ASP dataset. Rounded percentages indicating the amount of data represented in each bin (of size 0.1) are placed above each bar.

4.4 Dataset statistics

To summarize our datasets, we provide a numerical and statistical overview in Tables 1 and 2.

One factor we wanted to examine was the type of similarity that parallel branches exhibit; are their similarities surface-level or more linguistically complex? To measure this, we compute the *normalized lexical overlap* (NLO) of all pairs of related branches. Treating each branch as a multiset of tokens, we apply the formula

$$\text{NLO}(b_1, b_2) = \frac{|b_1 \cap b_2|}{|b_1 \cup b_2|}$$

where b_1, b_2 are related branches. This value is 1 if $b_1 = b_2$, and it is 0 if $b_1 \cap b_2 = \emptyset$.

In Fig. 3, we depict a histogram of the ASP dataset's NLO across all related branch pairs. (The PSE-I dataset's histogram is similar, but it peaks between 0.2 and 0.3 and has few pairs between 0 and 0.1.) This histogram shows that the vast majority of related branch pairs are frequently lexically dissimilar from one another; most are below 0.6 NLO, showing that it is very common to have at least half the words in a parallelism be different from one another. Thus, as our task definition asserted, parallelisms exploit many linguistic features to produce an effect; in turn, any method for RPD should try to capture these relationships.

5 Evaluation Metrics

Next, we describe a general family of evaluation metrics for RPD and specify one instance of it.

Suppose that we have a document **w**, as above, and a reference set **G** and a hypothesis set **H** of parallelisms in **w**. An evaluation metric for RPD should check both that the branches in **H** have the same spans as those in **G** and that the branches are grouped into parallelisms in **H** as they are in **G**.

Given these criteria, we follow prior work in coreference resolution (CR) to establish our metrics. Coreference resolution involves detecting an entity of interest and linking all mentions related to that entity together; in a similar manner, our task links a set of spans together. As in the Constrained Entity-Alignment F-Measure metrics (Luo, 2005), we express our metrics as a bipartite matching between **G** and **H**. We use the Kuhn-Munkres (also known as "Hungarian") algorithm (Kuhn, 1955; Munkres, 1957) to maximally align parallelisms between **G** and **H**. To do this, we must define two functions: score and size.

The function $\text{score}(p_1, p_2)$, where p_1 and p_2 are parallelisms, determines how well p_1 matches p_2, and the function $\text{size}(p)$, where p is a parallelism, bounds the score that p can merit with another parallelism. These functions must satisfy $\text{size}(p) > 0$ and $0 \leq \text{score}(p_1, p_2) \leq \min\{\text{size}(p_1), \text{size}(p_2)\}$.

With those in place, we can find the bipartite matching with maximum weight m,

$$m = \max_M \sum_{(p_1, p_2) \in M} \text{score}(p_1, p_2)$$

where the maximization is over matchings M between **G** and **H**. Having m, we define metrics in the likeness of precision (P), recall (R), and the F_1-score (F_1) as follows:

$$P = \frac{m}{\sum_{p \in \mathbf{H}} \text{size}(p)}$$
$$R = \frac{m}{\sum_{p \in \mathbf{G}} \text{size}(p)}$$
$$F_1 = \frac{2}{1/P + 1/R}.$$

The simplest choice of size and score is

$$\text{size}(p) = 1$$
$$\text{score}(p_1, p_2) = \begin{cases} 1 & \text{if } p_1 = p_2 \\ 0 & \text{if } p_1 \neq p_2. \end{cases}$$

We call this the *exact parallelism match* (EPM) metric, where each parallelism in **H** must perfectly match one in **G** to gain credit.

As an example of this metric, consider the passage given in Fig. 4. Suppose that the depicted parallelism—call it p_1—is the *only* parallelism in **G**. Furthermore, suppose that the model proposes two hypotheses, $\mathbf{H} = \{p_1, p_2\}$, where p_2 is a parallelism that does not overlap with p_1. Then

$$\text{score}(p_1, p_1) = 1 \qquad \text{score}(p_1, p_2) = 0$$

From this, we derive the maximally-weighted matching, $M = \{(p_1, p_1)\}$, and $m = 1$. Then

$$P = \frac{1}{2} \qquad R = \frac{1}{1} \qquad F_1 = \frac{2}{3}.$$

Appendix B introduces some alternative choices of `score` and `size` that give partial credit for imperfectly-matching hypothesized parallelisms.[7]

6 Models

In this section, we propose some models for automatic RPD as a starting point for future research. Our models here treat RPD as a sequence labeling problem, using several novel variants of BIO tagging (Ramshaw and Marcus, 1995).[8]

6.1 Tagging schemes

Branches are substrings, like named entities in NER, and parallelisms are sets of related substrings, like disfluencies in DD. Variants of BIO tagging have been successful for these sequence labeling tasks (Zayats et al., 2016; Reimers and Gurevych, 2017), so they are a natural choice for RPD as well. In this scheme, the first word of a branch is tagged B; the other words of a branch are tagged I; words outside of branches are tagged O.

However, BIO tagging does not indicate which branches are parallel with which. In each parallelism, for each branch b except the first, we augment the B tags with a *link*, which is a number that indicates the previous branch with which b is parallel. We propose two linking schemes.

Suppose we have consecutive parallel branches $b_1 = (i_1, j_1)$ and $b_2 = (i_2, j_2)$ with $j_1 < i_2$. A *token distance* link, akin to links used in DD (Hough and Schlangen, 2015), is $j_1 - i_2$; it is the (negative)

---

[7]We accompany this paper with the `pyrallelism` library. It implements each of our metrics and provides sample formats for evaluating RPD. It is available on PyPI and at `https://github.com/Mythologos/pyrallelism`.

[8]Our main modeling and results repository is available at `https://github.com/Mythologos/Intro-RPD`. Our models are implemented in PyTorch (Paszke et al., 2019) and are initially based on code by Robert Guthrie (2017).

number of word-to-word hops to get from b_2's start to b_1's end. A *branch distance* link is the (negative) number of branch-to-branch hops to get from b_2 to b_1. If P contains the interlocking parallelisms $p_1 = \{(1, 3), (7, 9)\}$ and $p_2 = \{(4, 6), (10, 12)\}$, then the token distance between $(1, 3)$ and $(7, 9)$ is -4, while the branch distance is -2.

It is important to form tag sequences that help the model to learn better, diverging decisions from the dominant majority class O. Therefore, in addition to adding links, we include three additional tag types, each of which is exhibited in Fig. 4.

First, the M tag replaces O tags that occur for tokens that occur in the *middle* of consecutive branches in a parallelism. Lines 2 and 3 of Fig. 4 exhibit this: four non-branch tags become M instead of O because they are between related branches. This shift obstructs a model from predicting single-branch parallelisms by providing a separate pathway to seek linked branches, as O $\rightarrow$ Bℓ (where ℓ stands for a link) can never occur in the data.

Second, the E tag replaces branch-ending I tags to indicate the *end* of a branch. Adding this tag removes the I $\rightarrow$ O transition. This change may encourage a model to be more sensitive to a branch's endpoint; because most parallelisms are more than two tokens long, branches largely must transition from B to either I or E, and E must eventually be selected before returning to O.

Third, the J tag replaces I tags in non-initial branches, where an initial branch is the first branch of a parallelism that occurs in a document. When paired with M tags, J tags help to promote a sequence of transitions which do not include O as a likely candidate until two branches have concluded. While the second example of Figure 4 displays this, Figure 5 shows this behavior across ASP's entire training set. Treating a sequence of tags as a linear chain, we tally all node transition pairs. When compared to the BIO chain of tags (left), we can see that I $\rightarrow$ O no longer exists in the BIOMJ chain (right). Only non-initial branch tokens (*i.e.*, Bλ or J) can transition to O. Through its supported transitions, the altered tagset actively enforces the constraint that a parallelism must have at least two branches.

With these three new tags, we form eight tagsets—BIO, BIOE, BIOJ, BIOM, BIOJE, BIOME, BIOMJ, and BIOMJE—and apply each link type to them, forming sixteen tagging schemes. These tagging schemes constitute all parallelisms in each dataset: each level of nesting is an addi-

	quotidie	dicimus	hoc	,	et	quotidie	facimus	,	et	quotidie	fit		in	nobis	.
Latin	**quotidie**	**dicimus**	**hoc**	,	et	**quotidie**	**facimus**	,	et	**quotidie**	**fit**		**in**	**nobis**	.
English	Every day	we say	this	,	and	every day	we do [it]	,	and	every day	[it] is done		in	us	.
BIO-Token	B	I	I	O	O	B–3	I	O	O	B–3	I		I	I	O
BIOMJ-Token	B	I	I	M	M	B–3	J	M	M	B–3	J		J	J	O
BIOME-Branch	B	I	E	M	M	B–1	E	M	M	B–1	I		I	E	O

Figure 4: The example of Fig. 1 from ASP annotated with various tagging schemes. For line 1, bolded words are part of the parallelism, and all contiguous units represent branches. For line 2, items in brackets indicate words not directly present (but implied) in the original text. For lines 3–5, "Token" and "Branch" refer to link types.
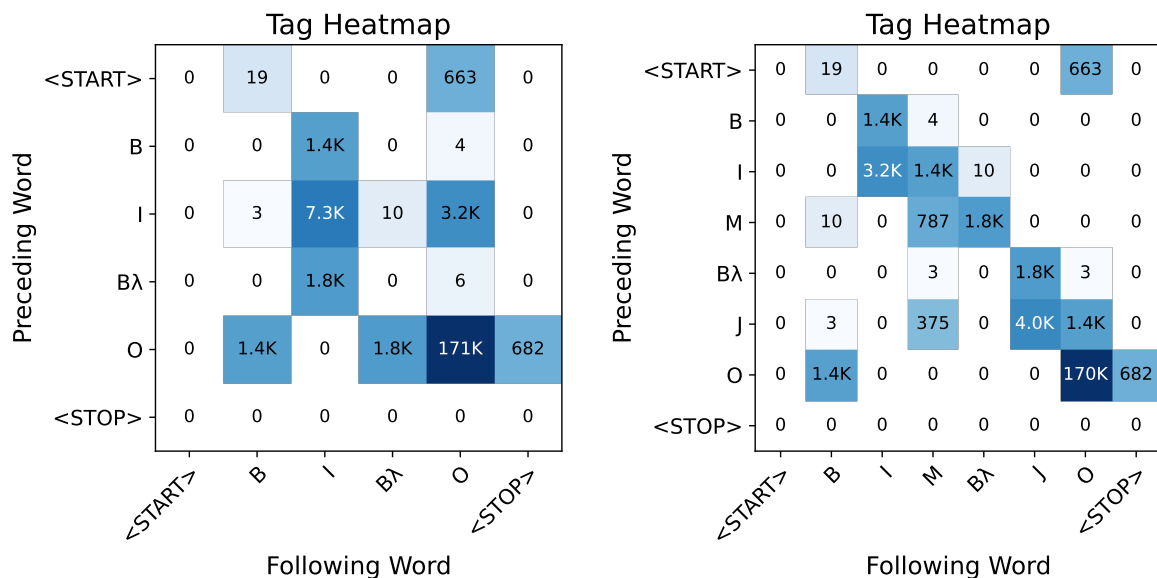

Figure 5: Two heatmaps tabulating tag transition frequencies across all (two) strata in ASP's training set. Darker colors indicate larger values; text colors change for readability. The <START> and <STOP> tokens refer to section beginnings and ends. The left and right heatmaps are for the BIO and BIOMJ tagsets, respectively.

tional layer, or *stratum* (pl. *strata*), of tags.

6.2 Architecture

Inspired by prior success in sequence labeling for named entity recognition, we employ a conditional random field (CRF) output layer (Lafferty et al., 2001) in combination with various neural networks (Huang et al., 2015; Ma and Hovy, 2016; Lample et al., 2016). Our general architecture (Fig. 6) proceeds in five steps. It *embeds* tokens (words or subwords) as vectors; it *blends* token-level embeddings into word-level embeddings; it *encodes* the sequence of embeddings to incorporate more contextual and task-specific information; it *maps* encodings to tag space with a linear layer; it uses a CRF to compute a distribution over tag sequences.

Each model examined in Section 7.2 is a variation on this paradigm. We tested a total of six models. Following work in NER, we selected a BiLSTM-CRF baseline (Huang et al., 2015; Ma and Hovy, 2016; Lample et al., 2016). We also tried exchanging the BiLSTM for a Transformer

(Vaswani et al., 2017) as an encoder layer.

We tried three embedding options. The first option was to learn embeddings from scratch. The second option was to use frozen word2vec embeddings (Mikolov et al., 2013). We selected a 300-dimensional embedding built from Latin data lemmatized by CLTK's `LatinBackoffLemmatizer` (Johnson et al., 2021) trained by Burns et al. (2021). The third option was to employ frozen embeddings from a BERT model—namely, Latin BERT (Bamman and Burns, 2020) for the ASP dataset and Chinese BERT with whole word masking (Cui et al., 2020, 2021) for the PSE-I dataset.

For both the Transformer encoder and the BERT embeddings, we applied WordPiece tokenization (Wu et al., 2016) by reusing the tokenizer previously trained for Latin BERT (Bamman and Burns, 2020) with the `tensor2tensor` library (Vaswani et al., 2018). We employed operations (termed *blending functions*) to combine subword representations into word representations. The choice of blending function did not heavily impact our

```
CRF
 ↑
Linear
 ↑
Encoder          {BiLSTM, Transformer, none}
 ↑
Blender          {take-first, sum, mean}
 ↑
Embedding        {learned, word2vec, BERT}
```
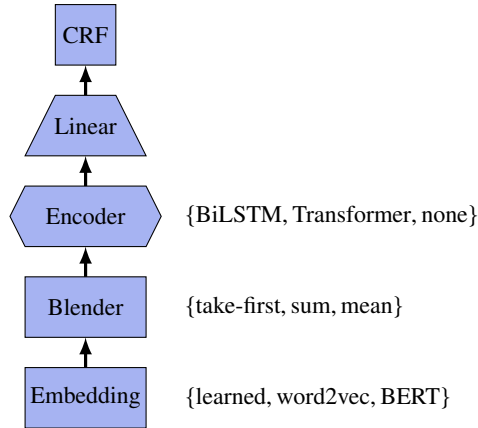
Figure 6: Generic Encoder-CRF architecture and per-level options examined. Shapes roughly indicate relative changes in representation sizes.

results, so we defer discussion of them to Appendix D.3. For other models, we did not use subwords, and no blending function was needed.

To reduce the average sequence length seen by our models, each sequence presented is a *section* rather than a whole document. For the ASP dataset, each sermon's division into sections was imposed by later editors of the texts. Meanwhile, for the PSE-I dataset, we split the data based on paragraph divisions. When sections remain longer than BERT's 512-token limit, we split sections into 512-token chunks and concatenate the output sequences after the embedding layer. As noted in previous CR work (Joshi et al., 2019), this approach is superior to merging overlapping chunks.

We discuss other design choices in Appendix D.

7 Experiments

In this section, we describe our experiments (Section 7.1 and present our results (Section 7.2).

7.1 Experimental design

For each dataset, we performed hyperparameter searches over several model architecture and tagging scheme combinations. We judged these as the elements which would likely primarily govern task performance. For the ASP dataset, we trained six possible architectures described in Section 6.2 with each of the sixteen tagging schemes described in Section 6.1. Meanwhile, for the PSE-I dataset, we ran the three BERT-based architectures with each of the same sixteen tagging schemes. The hyperparameters for each trial were chosen using random search (Bergstra and Bengio, 2012) described in Appendix F. Eight trials per configuration were

trained for the ASP and PSE-I datasets, totaling 768 and 384 experiments, respectively.

Each trial's model trained for up to 200 epochs using Adam (Kingma and Ba, 2015) and gradient clipping with an L_2 norm of 1 (Pascanu et al., 2013). We stopped training early if the model's F_1 score did not improve for 25 epochs on the validation set using the maximum branch-aware word overlap (MBAWO) metric (defined in Appendix B).[9] Each trial was assessed on the optimization set. We denoted the trial with the highest MBAWO score on this set per setting as that setting's best run. We evaluated each best run on the test set.

7.2 Results

To compare the performance across models, we determined the best result for each model, as shown in Table 3. "Best" is defined as the experiment with the highest F_1 score on the test set across all attempted settings. We also highlight a few factors which generally improved performance: the embeddings, encoders, and tagsets selected.[10]

In terms of *embeddings*, BERT embeddings vastly improved performance. As Table 5 depicts, BERT-based models exceeded every other non-BERT model by at least 0.2 F_1 on the ASP dataset. We attribute their superiority to the contextual representations produced by BERT. This is supported by the fact that both Burns et al.'s embeddings and Latin BERT's embeddings were mainly trained on the same Internet Archive dataset (Bamman and Crane, 2011; Bamman and Smith, 2012).

In terms of *tagging schemes*, we wanted to know whether any schemes performed significantly better than the others. We applied the Friedman ranked-sums test (Friedman, 1937, 1940). Although this test is usually used to compare multiple classifiers across multiple datasets (Demšar, 2006), we instead took results across a single dataset (ASP) and sampling procedure (our hyperparameter search process) and considered each collection of best model F_1 scores as a sample. Because the Friedman test is nonparametric, we circumvent issues arising from the fact that model performance already causes F_1 scores to differ heavily.

With $p < 0.05$, we find the differences between samples to be significant ($p < 0.001$). We then

---

[9]We opted for MBAWO instead of EPM because we were concerned that the stricter EPM metric would overly penalize incremental progress in capturing correct tokens.

[10]For an error analysis and a full catalogue of our results and best model hyperparameters, see Appendices G to I.

Dataset	Model Components		Tagging Scheme		Results		
	Embedding	Encoder	Tagset	Link Type	Precision	Recall	F_1
ASP	Learned (Word)	BiLSTM	BIO	Token	0.16	0.13	0.14
	word2vec	BiLSTM	BIOMJE	Branch	0.24	0.12	0.16
	Learned (Subword)	Transformer	BIOMJ	Token	0.06	0.07	0.07
	Latin BERT	–	BIOMJ	Token	**0.51**	0.33	**0.40**
	Latin BERT	BiLSTM	BIOMJ	Token	0.47	**0.34**	0.39
	Latin BERT	Transformer	BIOME	Branch	0.44	0.31	0.37
PSE-I	Chinese BERT	–	BIOM	Branch	0.30	0.42	0.35
	Chinese BERT	BiLSTM	BIOMJ	Token	0.38	**0.51**	**0.43**
	Chinese BERT	Transformer	BIOME	Token	**0.40**	0.36	0.38

Table 3: Best test set results, rounded to the second decimal place, on our datasets according to the EPM metric for each Encoder-CRF configuration. The best result in each column is written in boldface.

Tagset	Link	Avg. Rank (↓)
BIO	Token	9.17
	Branch	9.92
BIOE	Token	9.83
	Branch	12.75
BIOJ	Token	11.83
	Branch	11.08
BIOM	Token	6.83
	Branch	6.50
BIOJE	Token	11.00
	Branch	13.25
BIOME	Token	9.17
	Branch	4.67
BIOMJ	Token	**3.33**
	Branch	4.33
BIOMJE	Token	5.50
	Branch	6.83

Table 4: Average rank of each tagging scheme's best model for all architectures across the ASP test set. The lowest (*i.e.*, best) result is bolded.

Embedding + Encoder	F_1 (ASP)	F_1 (PSE-I)
Learned (W) + BiLSTM	0.08 ± 0.03	–
word2vec + BiLSTM	0.08 ± 0.03	–
Learned (SW) + Transformer	0.02 ± 0.02	–
BERT	0.26 ± 0.07	0.24 ± 0.07
BERT + BiLSTM	0.32 ± 0.04	0.36 ± 0.04
BERT + Transformer	0.28 ± 0.05	0.30 ± 0.05

Table 5: Best test set result averages over each Encoder-CRF configuration for EPM. "W" and "SW" stand for "word" and "subword", respectively. The BERT version used corresponds to each dataset's language.

used a post-hoc Nemenyi test (Nemenyi, 1963) via the `scikit-posthocs` library (Terpilowski, 2019) to determine which tagging scheme pairs achieve significantly different results. With $p < 0.05$, only one pair of tagging schemes significantly differs: BIOMJ-TD and BIOJE-BD—the best and worst schemes, according to the average ranks of each scheme's F_1 scores (as presented in Table 4). Given our low sample count, we suspect that further samples might show the superiority of certain schemes. With this in mind, we tentatively recommend any M-based tagging schemes, especially in combination with either of the E or J tags, for use.

In terms of *encoders*, BiLSTMs generally outperformed Transformers. Although non-BiLSTM models achieved peak performance in Table 3, the average performance by BiLSTMs was consistently higher. Table 5 depicts this regardless of the type of embedding used: each BiLSTM model performs

on average better than its Transformer (or encoder-less) variant. One possible reason for BiLSTMs' superiority may be that the subtask of predicting distance-based links benefits from LSTMs' ability to count (Weiss et al., 2018; Suzgun et al., 2019b,a).

8 Conclusions and Future Work

In this paper, we introduced the task of rhetorical parallelism detection. We described two datasets, an evaluation framework, and several baseline models for the task. Our baselines achieved fairly good performance, and we found that BERT embeddings, a BiLSTM-based encoder, and an M-inclusive tagging scheme were valuable modeling components.

We identify a few directions for future work. The models described here have a closed tagset, so they cannot predict links for distances not seen in the training data; modeling links in other ways might be more effective. Our models only predict flat parallelisms; approaches for nested NER (Finkel and Manning, 2009; Wang et al., 2020) may be a viable direction for extending the Encoder-CRF paradigm toward this end. Finally, applying this work's methods to detect grammatical parallelism might enhance tasks like syntactic parsing, automated essay evaluation, or disfluency detection.

9 Limitations

This work introduces a novel task in the form of rhetorical parallelism detection (RPD). Because it is novel, it is innately exploratory. Although it establishes approaches for building and organizing datasets, for evaluating performance at various granularities, and for constructing models to capture parallel structure, it does not do all these perfectly. Thus, it should not be the last word on the topic. In the following paragraphs, we highlight elements of this work which could be improved.

First, this work puts forth two datasets for RPD: the Augustinian Sermon Parallelism (ASP) and the Paibi Student Essay (PSE) (Song et al., 2016) datasets. We annotated both datasets—the former from scratch and the latter on the basis of prior annotations. As is noted in Appendix C, our annotation scheme was not perfect.

- For the ASP dataset, we achieved a 0.4124 EPM F_1 score (although higher branch-based and word-based scores) between our two annotators on bootstrapping experiments. Our scores indicate moderate agreement, but the meaningful disagreement implies that our guidelines could be sharpened.

- For the PSE-I dataset—the version of the PSE dataset including our annotations—we did not perform an inter-annotator agreement study. We did not consider it necessary because we were already overlapping with prior annotators' conclusions, but one could argue that the sentence- and span-level annotation tasks differ enough to warrant separate studies.

Second, regarding the ASP dataset, we acknowledge that the use of Latin as a foundation for this task limits its immediate applicability to modern NLP contexts. We believe that the ASP dataset is readily applicable to tasks such as authorship attribution and authorship authentication, which both have precedent in Latin (Forstall and Scheirer, 2010; Kestemont et al., 2016; Kabala, 2020; Corbara et al., 2023) and frequently employ stylistic features in their approaches. Moreover, we believe that ASP can aid distant reading approaches (Moretti, 2000; Jockers, 2013) in permitting the annotation of large corpora with stylistic annotations.

On the other hand, the inclusion of the PSE dataset for RPD provides a modern language for which this task is available. Moreover, late into this work, we became aware of a vein of literature

that could either add to the available Chinese data based on an interest in parallelism detection as a sentence-level or clause-level subtask (Xu et al., 2021; Zhu et al., 2022) as well as work performing narrower, more restricted versions of word-level parallelism detection (Gawryjolek, 2009) or chiasmus detection (Dubremetz and Nivre, 2015, 2018), in English. Future work can potentially expand RPD to the datasets provided by these works.

Third, some modeling decisions were made to suit the needs of our problem and provide baselines without exploring the larger space of possibilities. Namely, as described in Section 6.2 and Appendix D.3, we use a blending function to combine subwords into words so that the appropriate number of tags would be produced. However, we could have also eschewed the CRF altogether and attempted to follow BERT in selecting every word's first tag as its representative tag (Devlin et al., 2019). Future work could further and more deeply investigate the search space of model architectures to improve performance on this task.

Acknowledgements

References

Tosin Adewumi, Roshanak Vadoodi, Aparajita Tripathy, Konstantina Nikolaido, Foteini Liwicki, and Marcus Liwicki. 2022. Potential idiomatic expression (PIE)-English: Corpus for classes of idioms. In *Proceedings of the Thirteenth Language Resources and Evaluation Conference*, pages 689–696, Marseille, France. European Language Resources Association.

Mohammed Alliheedi. 2012. Multi-document Summarization System Using Rhetorical Information. Master's thesis, University of Waterloo, Waterloo, Ontario, Canada.

Ron Artstein and Massimo Poesio. 2008. Survey article: Inter-coder agreement for computational linguistics. *Computational Linguistics*, 34(4):555–596.

Saint Augustine of Hippo. 1995. *De doctrina Christiana*. Oxford Early Christian texts. Clarendon, Oxford.

Saint Augustine of Hippo. 2000a. *Sermones: Part 1*, volume 12 of *Saint Augustine: Opera Omnia - Corpus Augustinianum Gissense. Electronic Edition*. InteLex Corp., Charlottesville, Virginia, U.S.A.

Saint Augustine of Hippo. 2000b. *Sermones: Part 2*, volume 13 of *Saint Augustine: Opera Omnia - Corpus Augustinianum Gissense. Electronic Edition*. InteLex Corp., Charlottesville, Virginia, U.S.A.

Jimmy Lei Ba, Jamie Ryan Kiros, and Geoffrey E. Hinton. 2016. Layer normalization. arXiv:1607.06450.

David Bamman and Patrick J. Burns. 2020. Latin BERT: A contextual language model for classical philology. ArXiv:2009.10053.

David Bamman and Gregory Crane. 2011. Measuring historical word sense variation. In *Proceedings of the 11th Annual International ACM/IEEE Joint Conference on Digital Libraries*, JCDL '11, pages 1–10, New York, NY, USA. Association for Computing Machinery.

David Bamman and David Smith. 2012. Extracting two thousand years of Latin from a million book library. *Journal on Computing and Cultural Heritage*, 5(1).

Beata Beigman Klebanov and Nitin Madnani. 2020. Automated evaluation of writing – 50 years and counting. In *Proceedings of the 58th Annual Meeting of the Association for Computational Linguistics*, pages 7796–7810, Online. Association for Computational Linguistics.

James Bergstra and Yoshua Bengio. 2012. Random search for hyper-parameter optimization. *J. Mach. Learn. Res.*, 13:281–305.

Patrick J. Burns, James A. Brofos, Kyle Li, Pramit Chaudhuri, and Joseph P. Dexter. 2021. Profiling of intertextuality in Latin literature using word embeddings. In *Proceedings of the 2021 Conference of the North American Chapter of the Association for Computational Linguistics: Human Language Technologies*, pages 4900–4907, Online. Association for Computational Linguistics.

Jean Carletta. 1996. Assessing agreement on classification tasks: The kappa statistic. *Computational Linguistics*, 22(2):249–254.

Noe Casas, Marta R. Costa-jussà, and José A. R. Fonollosa. 2020. Combining subword representations into word-level representations in the Transformer architecture. In *Proceedings of the 58th Annual Meeting of the Association for Computational Linguistics: Student Research Workshop*, pages 66–71, Online. Association for Computational Linguistics.

Wanxiang Che, Zhenghua Li, and Ting Liu. 2010. LTP: A Chinese language technology platform. In *Coling 2010: Demonstrations*, pages 13–16, Beijing, China. Coling 2010 Organizing Committee.

Mia Xu Chen, Orhan Firat, Ankur Bapna, Melvin Johnson, Wolfgang Macherey, George Foster, Llion Jones, Mike Schuster, Noam Shazeer, Niki Parmar, Ashish Vaswani, Jakob Uszkoreit, Lukasz Kaiser, Zhifeng Chen, Yonghui Wu, and Macduff Hughes. 2018. The best of both worlds: Combining recent advances in neural machine translation. In *Proceedings of the 56th Annual Meeting of the Association for Computational Linguistics (Volume 1: Long Papers)*, pages 76–86, Melbourne, Australia. Association for Computational Linguistics.

Stanley F. Chen and Joshua Goodman. 1998. An empirical study of smoothing techniques for language modeling. Technical Report TR-10-98, Harvard University, Cambridge, Massachusetts.

Jacob Cohen. 1960. A coefficient of agreement for nominal scales. *Educational and Psychological Measurement*, 20(1):37–46.

Silvia Corbara, Alejandro Moreo, and Fabrizio Sebastiani. 2023. Syllabic quantity patterns as rhythmic features for Latin authorship attribution. *Journal of the Association for Information Science and Technology*, 74(1):128–141.

Yiming Cui, Wanxiang Che, Ting Liu, Bing Qin, Shijin Wang, and Guoping Hu. 2020. Revisiting pre-trained models for Chinese natural language processing. In *Proceedings of the 2020 Conference on Empirical Methods in Natural Language Processing: Findings*, pages 657–668, Online. Association for Computational Linguistics.

Yiming Cui, Wanxiang Che, Ting Liu, Bing Qin, and Ziqing Yang. 2021. Pre-training with whole word masking for Chinese BERT. *IEEE Transactions on Audio, Speech and Language Processing*.

Yange Dai, Wei Song, Xianjun Liu, Lizhen Liu, and Xinlei Zhao. 2018. Recognition of parallelism sentence based on recurrent neural network. In *2018 IEEE 9th International Conference on Software Engineering and Service Science (ICSESS)*, pages 148–151.

Janez Demšar. 2006. Statistical comparisons of classifiers over multiple data sets. *Journal of Machine Learning Research*, 7(1):1–30.

Jacob Devlin, Ming-Wei Chang, Kenton Lee, and Kristina Toutanova. 2019. BERT: Pre-training of deep bidirectional Transformers for language understanding. In *Proceedings of the 2019 Conference of the North American Chapter of the Association for Computational Linguistics: Human Language Technologies, Volume 1 (Long and Short Papers)*, pages 4171–4186, Minneapolis, Minnesota. Association for Computational Linguistics.

Marie Dubremetz and Joakim Nivre. 2015. Rhetorical figure detection: The case of chiasmus. In *Proceedings of the Fourth Workshop on Computational Linguistics for Literature*, pages 23–31, Denver, Colorado, USA. Association for Computational Linguistics.

Marie Dubremetz and Joakim Nivre. 2018. Rhetorical figure detection: Chiasmus, epanaphora, epiphora. *Frontiers in Digital Humanities*, 5.

Jenny Rose Finkel and Christopher D. Manning. 2009. Nested named entity recognition. In *Proceedings of the 2009 Conference on Empirical Methods in Natural Language Processing*, pages 141–150, Singapore. Association for Computational Linguistics.

Christopher Forstall and Walter Scheirer. 2010. Features from frequency: Authorship and stylistic analysis using repetitive sound. *Journal of the Chicago Colloquium on Digital Humanities and Computer Science*, 1(2).

Milton Friedman. 1937. The use of ranks to avoid the assumption of normality implicit in the analysis of variance. *Journal of the American Statistical Association*, 32(200):675–701.

Milton Friedman. 1940. A comparison of alternative tests of significance for the problem of *m* rankings. *The Annals of Mathematical Statistics*, 11(1):86–92.

Akansha Gautam and Koteswar Rao Jerripothula. 2020. SGG: Spinbot, Grammarly and GloVe based fake news detection. In *2020 IEEE Sixth International Conference on Multimedia Big Data (BigMM)*, pages 174–182.

Jakub Jan Gawryjolek. 2009. Automated annotation and visualization of rhetorical figures. Master's thesis, University of Waterloo, Waterloo, Ontario, Canada.

Kallirroi Georgila. 2009. Using integer linear programming for detecting speech disfluencies. In *Proceedings of Human Language Technologies: The 2009 Annual Conference of the North American Chapter of the Association for Computational Linguistics, Companion Volume: Short Papers*, pages 109–112, Boulder, Colorado. Association for Computational Linguistics.

Jiefu Gong, Xiao Hu, Wei Song, Ruiji Fu, Zhichao Sheng, Bo Zhu, Shijin Wang, and Ting Liu. 2021. IFlyEA: A Chinese essay assessment system with automated rating, review generation, and recommendation. In *Proceedings of the 59th Annual Meeting of the Association for Computational Linguistics and the 11th International Joint Conference on Natural Language Processing: System Demonstrations*, pages 240–248, Online. Association for Computational Linguistics.

Marie Guégan and Nicolas Hernandez. 2006. Recognizing textual parallelisms with edit distance and similarity degree. In *11th Conference of the European Chapter of the Association for Computational Linguistics*, pages 281–288, Trento, Italy. Association for Computational Linguistics.

Robert Guthrie. 2017. DeepLearningForNLPInPytorch: An IPython Notebook tutorial on deep learning for natural language processing, including structure prediction.

Dan Hendrycks and Kevin Gimpel. 2016. Gaussian error linear units (GELUs). arXiv:1606.08415.

Julian Hough and David Schlangen. 2015. Recurrent neural networks for incremental disfluency detection. In *Proc. Interspeech 2015*, pages 849–853.

George Hripcsak and Adam S. Rothschild. 2005. Agreement, the f-measure, and reliability in information retrieval. *Journal of the American Medical Informatics Association : JAMIA*, 12(3):296–298.

Zhiheng Huang, Wei Xu, and Kai Yu. 2015. Bidirectional LSTM-CRF models for sequence tagging. *CoRR*, abs/1508.01991.

Matthew Lee Jockers. 2013. *Macroanalysis: Digital Methods and Literary History*. Topics in the Digital Humanities. University of Illinois Press, Urbana.

Kyle P. Johnson, Patrick J. Burns, John Stewart, Todd Cook, Clément Besnier, and William J. B. Mattingly. 2021. The Classical Language Toolkit: An NLP framework for pre-modern languages. In *Proceedings of the 59th Annual Meeting of the Association for Computational Linguistics and the 11th International Joint Conference on Natural Language Processing: System Demonstrations*, pages 20–29, Online. Association for Computational Linguistics.

Mandar Joshi, Omer Levy, Luke Zettlemoyer, and Daniel Weld. 2019. BERT for coreference resolution: Baselines and analysis. In *Proceedings of the 2019 Conference on Empirical Methods in Natural Language Processing and the 9th International Joint Conference on Natural Language Processing (EMNLP-IJCNLP)*, pages 5803–5808, Hong Kong, China. Association for Computational Linguistics.

Jakub Kabala. 2020. Computational authorship attribution in medieval Latin corpora: The case of the Monk of Lido (ca. 1101–08) and Gallus Anonymous (ca. 1113–17). *Language Resources and Evaluation*, 54(1):25–56.

Zixuan Ke and Vincent Ng. 2019. Automated essay scoring: A survey of the state of the art. In *Proceedings of the Twenty-Eighth International Joint Conference on Artificial Intelligence, IJCAI-19*, pages 6300–6308. International Joint Conferences on Artificial Intelligence Organization.

Mike Kestemont, Justin Stover, Moshe Koppel, Folgert Karsdorp, and Walter Daelemans. 2016. Authenticating the writings of Julius Caesar. *Expert Systems with Applications*, 63:86–96.

Diederik P. Kingma and Jimmy Ba. 2015. Adam: A method for stochastic optimization. In *3rd International Conference on Learning Representations, ICLR 2015, San Diego, CA, USA, May 7-9, 2015, Conference Track Proceedings*.

Klaus Krippendorff. 2019. *Reliability*, fourth edition, chapter 12. SAGE Publications, Inc., Thousand Oaks.

H. W. Kuhn. 1955. The Hungarian method for the assignment problem. *Naval Research Logistics Quarterly*, 2(1-2):83–97.

John Lafferty, Andrew McCallum, and Fernando Pereira. 2001. Conditional random fields: Probabilistic models for segmenting and labeling sequence data. *Departmental Papers (CIS)*.

Guillaume Lample, Miguel Ballesteros, Sandeep Subramanian, Kazuya Kawakami, and Chris Dyer. 2016. Neural architectures for named entity recognition. In *Proceedings of the 2016 Conference of the North American Chapter of the Association for Computational Linguistics: Human Language Technologies*, pages 260–270, San Diego, California. Association for Computational Linguistics.

J. Richard Landis and Gary G. Koch. 1977. The measurement of observer agreement for categorical data. *Biometrics*, 33(1):159–174.

Guanghui Liu, Lijun Fu, Bo Yu, and Li Cui. 2022. Automatic recognition of parallel sentence based on sentences-interaction CNN and its application. In *2022 7th International Conference on Computer and Communication Systems (ICCCS)*, pages 245–250.

Xiaoqiang Luo. 2005. On coreference resolution performance metrics. In *Proceedings of Human Language Technology Conference and Conference on Empirical Methods in Natural Language Processing*, pages 25–32, Vancouver, British Columbia, Canada. Association for Computational Linguistics.

Xuezhe Ma and Eduard Hovy. 2016. End-to-end sequence labeling via bi-directional LSTM-CNNs-CRF. In *Proceedings of the 54th Annual Meeting of the Association for Computational Linguistics (Volume 1: Long Papers)*, pages 1064–1074, Berlin, Germany. Association for Computational Linguistics.

Marie W. Meteer and Ann A. Taylor. 1995. Dysfluency annotation stylebook for the Switchboard corpus.

Tomás Mikolov, Kai Chen, Greg Corrado, and Jeffrey Dean. 2013. Efficient estimation of word representations in vector space. In *1st International Conference on Learning Representations, ICLR 2013, Scottsdale, Arizona, USA, May 2-4, 2013, Workshop Track Proceedings*.

Franco Moretti. 2000. Conjectures on world literature. *New Left Review*, 1(1):54–68.

James Munkres. 1957. Algorithms for the assignment and transportation problems. *Journal of the Society for Industrial and Applied Mathematics*, 5(1):32–38.

Peter Bjorn Nemenyi. 1963. *Distribution-Free Multiple Comparisons*. Ph.D. thesis, Princeton University, Princeton, New Jersey, USA.

Hermann Ney, Ute Essen, and Reinhard Kneser. 1994. On structuring probabilistic dependences in stochastic language modelling. *Computer Speech & Language*, 8(1):1–38.

Toan Q. Nguyen and Julian Salazar. 2019. Transformers without tears: Improving the normalization of self-attention. In *Proceedings of the 16th International Conference on Spoken Language Translation*, Hong Kong. Association for Computational Linguistics.

Mari Ostendorf and Sangyun Hahn. 2013. A sequential repetition model for improved disfluency detection. In *Proc. Interspeech 2013*, pages 2624–2628.

Ellis B. Page. 1966. The imminence of . . . grading essays by computer. *The Phi Delta Kappan*, 47(5):238–243.

Razvan Pascanu, Tomas Mikolov, and Yoshua Bengio. 2013. On the difficulty of training recurrent neural networks. In *Proceedings of the 30th International Conference on Machine Learning*, volume 28 of *Proceedings of Machine Learning Research*, pages 1310–1318, Atlanta, Georgia, USA. PMLR.

Adam Paszke, Sam Gross, Francisco Massa, Adam Lerer, James Bradbury, Gregory Chanan, Trevor Killeen, Zeming Lin, Natalia Gimelshein, Luca Antiga, Alban Desmaison, Andreas Kopf, Edward Yang, Zachary DeVito, Martin Raison, Alykhan Tejani, Sasank Chilamkurthy, Benoit Steiner, Lu Fang, Junjie Bai, and Soumith Chintala. 2019. PyTorch: An imperative style, high-performance deep learning library. In H. Wallach, H. Larochelle, A. Beygelzimer, F. dAlché-Buc, E. Fox, and R. Garnett, editors, *Advances in Neural Information Processing Systems 32*, pages 8024–8035. Curran Associates, Inc.

Lance Ramshaw and Mitch Marcus. 1995. Text chunking using transformation-based learning. In *Third Workshop on Very Large Corpora*, pages 82–94.

Nils Reimers and Iryna Gurevych. 2017. Reporting score distributions makes a difference: Performance study of LSTM-networks for sequence tagging. In *Proceedings of the 2017 Conference on Empirical Methods in Natural Language Processing*, pages 338–348, Copenhagen, Denmark. Association for Computational Linguistics.

Elizabeth Shriberg. 1994. *Preliminaries to a Theory of Speech Disfluencies*. Ph.D. thesis, University of California, Berkeley, Berkeley, California, USA.

Wei Song, Tong Liu, Ruiji Fu, Lizhen Liu, Hanshi Wang, and Ting Liu. 2016. Learning to identify sentence parallelism in student essays. In *Proceedings of COLING 2016, the 26th International Conference on Computational Linguistics: Technical Papers*, pages 794–803, Osaka, Japan. The COLING 2016 Organizing Committee.

Fábio Souza, Rodrigo Frassetto Nogueira, and Roberto de Alencar Lotufo. 2019. Portuguese named entity recognition using BERT-CRF. arXiv:1909.10649.

Pontus Stenetorp, Sampo Pyysalo, Goran Topić, Tomoko Ohta, Sophia Ananiadou, and Jun'ichi Tsujii. 2012. BRAT: A web-based tool for NLP-assisted text annotation. In *Proceedings of the Demonstrations Session at EACL 2012*, Avignon, France. Association for Computational Linguistics.

Gaius Suetonius Tranquillus. 1993. *De Vita Caesarum Libri VIII*, volume 1 of *Opera*. B. G. Teubner.

Mirac Suzgun, Yonatan Belinkov, Stuart Shieber, and Sebastian Gehrmann. 2019a. LSTM networks can perform dynamic counting. In *Proceedings of the Workshop on Deep Learning and Formal Languages: Building Bridges*, pages 44–54, Florence. Association for Computational Linguistics.

Mirac Suzgun, Yonatan Belinkov, and Stuart M. Shieber. 2019b. On evaluating the generalization of LSTM models in formal languages. In *Proceedings of the Society for Computation in Linguistics (SCiL) 2019*, pages 277–286.

Chenhao Tan, Hao Peng, and Noah A. Smith. 2018. "You are no Jack Kennedy": On media selection of highlights from presidential debates. In *Proceedings of the 2018 World Wide Web Conference*, WWW '18, pages 945–954, Republic and Canton of Geneva, CHE. International World Wide Web Conferences Steering Committee.

Maksim Terpilowski. 2019. scikit-posthocs: Pairwise multiple comparison tests in Python. *The Journal of Open Source Software*, 4(36):1169.

Ashish Vaswani, Samy Bengio, Eugene Brevdo, Francois Chollet, Aidan N. Gomez, Stephan Gouws, Llion Jones, Łukasz Kaiser, Nal Kalchbrenner, Niki Parmar, Ryan Sepassi, Noam Shazeer, and Jakob Uszkoreit. 2018. Tensor2Tensor for neural machine translation. *CoRR*, abs/1803.07416.

Ashish Vaswani, Noam Shazeer, Niki Parmar, Jakob Uszkoreit, Llion Jones, Aidan N. Gomez, Łukasz Kaiser, and Illia Polosukhin. 2017. Attention is all you need. In *Advances in Neural Information Processing Systems*, volume 30. Curran Associates, Inc.

Pauli Virtanen, Ralf Gommers, Travis E. Oliphant, Matt Haberland, Tyler Reddy, David Cournapeau, Evgeni Burovski, Pearu Peterson, Warren Weckesser, Jonathan Bright, Stéfan J. van der Walt, Matthew Brett, Joshua Wilson, K. Jarrod Millman, Nikolay Mayorov, Andrew R. J. Nelson, Eric Jones, Robert Kern, Eric Larson, C J Carey, İlhan Polat, Yu Feng, Eric W. Moore, Jake VanderPlas, Denis Laxalde, Josef Perktold, Robert Cimrman, Ian Henriksen, E. A. Quintero, Charles R. Harris, Anne M. Archibald, Antônio H. Ribeiro, Fabian Pedregosa, Paul van Mulbregt, and SciPy 1.0 Contributors. 2020. SciPy 1.0: Fundamental algorithms for scientific computing in Python. *Nature Methods*, 17:261–272.

Jue Wang, Lidan Shou, Ke Chen, and Gang Chen. 2020. Pyramid: A layered model for nested named entity recognition. In *Proceedings of the 58th Annual Meeting of the Association for Computational Linguistics*, pages 5918–5928, Online. Association for Computational Linguistics.

Qiang Wang, Bei Li, Tong Xiao, Jingbo Zhu, Changliang Li, Derek F. Wong, and Lidia S. Chao. 2019. Learning deep Transformer models for machine translation. In *Proceedings of the 57th Annual Meeting of the Association for Computational Linguistics*, pages 1810–1822, Florence, Italy. Association for Computational Linguistics.

Gail Weiss, Yoav Goldberg, and Eran Yahav. 2018. On the practical computational power of finite precision RNNs for language recognition. In *Proceedings of the 56th Annual Meeting of the Association for Computational Linguistics (Volume 2: Short Papers)*, pages 740–745, Melbourne, Australia. Association for Computational Linguistics.

Yonghui Wu, Mike Schuster, Zhifeng Chen, Quoc V. Le, Mohammad Norouzi, Wolfgang Macherey, Maxim Krikun, Yuan Cao, Qin Gao, Klaus Macherey, Jeff Klingner, Apurva Shah, Melvin Johnson, Xiaobing Liu, Lukasz Kaiser, Stephan Gouws, Yoshikiyo Kato, Taku Kudo, Hideto Kazawa, Keith Stevens, George Kurian, Nishant Patil, Wei Wang, Cliff Young, Jason Smith, Jason Riesa, Alex Rudnick, Oriol Vinyals, Greg Corrado, Macduff Hughes, and Jeffrey Dean. 2016. Google's neural machine translation system: Bridging the gap between human and machine translation. arXiv:1609.08144.

Guowei Xu, Wenbiao Ding, Weiping Fu, Zhongqin Wu, and Zitao Liu. 2021. Robust learning for text classification with multi-source noise simulation and hard example mining. In *Machine Learning and Knowledge Discovery in Databases. Applied Data Science Track*, pages 285–301, Cham. Springer International Publishing.

Vicky Zayats and Mari Ostendorf. 2019. Giving attention to the unexpected: Using prosody innovations in disfluency detection. In *Proceedings of the 2019 Conference of the North American Chapter of the Association for Computational Linguistics: Human Language Technologies, Volume 1 (Long and Short Papers)*, pages 86–95, Minneapolis, Minnesota. Association for Computational Linguistics.

Vicky Zayats, Mari Ostendorf, and Hannaneh Hajishirzi. 2016. Disfluency detection using a bidirectional LSTM. In *Proc. Interspeech 2016*, pages 2523–2527.

Victoria Zayats, Mari Ostendorf, and Hannaneh Hajishirzi. 2014. Multi-domain disfluency and repair detection. In *Proc. Interspeech 2014*, pages 2907–2911.

Dawei Zhu, Qiusi Zhan, Zhejian Zhou, Yifan Song, Jiebin Zhang, and Sujian Li. 2022. ConFiguRe: Exploring discourse-level Chinese figures of speech. In

A Annotation Procedures

In Section 2, we described two major guidelines which directed our study of parallel structures. Here, we list the specific criteria which were used by our annotators to locate parallelisms. Moreover, we describe our annotation scheme in more detail. We begin by enumerating general criteria in Appendix A.1 before discussing specific applications of these criteria in Appendix A.2.

A.1 General Guidelines

In general, branches of parallelisms were tagged from the first identical (or similar) word to the last identical (or similar) word; as such, each branch was maximally represented. Branches were detected, paired, and combined based upon whether they exhibited at least *two* of these criteria:

- They contained identical number of words (or were within approximately two words of one another).
- They had identical syntactic structure.
- They had two or more pairs of words of an identical grammatical form in identical order.
- They had two or more pairs of words that are lexically identical, are synonyms, are cognates, or are antonyms.
- They had at least two words that have a phonetically similar ending (*e.g.*, rhyme).
- They were a short distance from one another (*i.e.*, they had few intervening words). The acceptable margin was again around two words.

A.2 Specific Applications

As mentioned earlier, we used the BRAT annotation tool (Stenetorp et al., 2012) to form our datasets.

For the ASP dataset, we developed an annotation scheme consisting of BRAT's entities and relationships. An entity could be a ParallelArm or one of ChiasmA and ChiasmB. A relationship could be Parallel, linking two ParallelArm entities. This relationship indicates a synchystic parallel structure. A relationship could also be Chiasm, linking a ChiasmA and a ChiasmB and labeling a chiastic structure. Our two annotators, both for the initial data collection and the inter-annotator agreement

study (see Appendix C), could nest annotations; however, they could not overlap them.

Meanwhile, for the PSE-I dataset, we made a few changes. Because we were mostly interested in annotating sentences that were already marked as parallel in the dataset, we did away with the distinction between synchystic and chiastic parallelisms. Instead, all branches of a parallelism were tagged as Branch entities and connected with Parallel relationships. Annotators were also allowed to use a dummy entity type to tag sentences if they were deemed not to be parallel, but this was never done. The five annotators were told to focus on marked sentences in BRAT, but they were allowed to connect these sentences to unmarked sentences in the same paragraph if they noticed a parallelism.

B Additional Metrics

In Section 5, we constructed a framework for defining parallelism-related metrics. We defined one such metric for exact parallelism matches between parallelisms. However, the score and size functions allow for finer granularity. Below, we define three additional metrics which examine parallelisms in terms of their branches, their words-per-branch, and their words altogether.

First, we describe the *maximum parallel branch match* (MPBM) metric. MPBM focuses on branches. It retains a sense of parallel structure by requiring that at least two branches are shared between the hypothesis and reference parallelisms to produce any score. The functions of MPBM are:

$$\text{size}(p) = |p|$$
$$\text{score}(p_1, p_2) = \text{hasParBranch}(p_1, p_2) \cdot |p_1 \cap p_2|$$

where

$$\text{hasParBranch}(q, r) = \mathbb{I}[|q \cap r| \geq 2]$$

Next, we proceed to metrics which examine parallelisms in terms of their words (which we use interchangeably with tokens below). Let p be a parallelism. We define $\text{words}(p) = \bigcup_{(i,j) \in p} \{i, \ldots, j\}$ as the set of all token positions in branches; this formulation dissolves distinctions between branches for a parallelism. We also define $\text{branchedWords}(p) = \{\{i, \ldots, j\} : (i, j) \in p\}$ as the set of all token positions in branches divided up into a set per branch. This formulation preserves branch-level distinctions.

The first word-level metric is the *maximum branch-aware word overlap* (MBAWO) metric.

The objective of this metric is similar to MPBM: if at least two distinct branches are matched in a parallelism, then such a matching should obtain some score. However, this metric is less strict than MPBM in that only *words* from two distinct branches need to match. In short, if at least two branches in a hypothesis parallelism have words that match with at least two branches in a reference parallelism, then the match merits a nonzero score based on the number of tokens matched.

To compute this metric, we define $\mathcal{W}(p_1, p_2) =$ branchedWords$(p_1) \times$ branchedWords(p_2); that is, $\mathcal{W}$ pairs all branches of one parallelism with all branches of another parallelism in terms of their word indices. Then we define `score` and `size` as:

$$\texttt{size}(p) = |\text{words}(p)|$$

$$\texttt{score}(p_1, p_2) = \max_{W \in \mathcal{W}(p_1, p_2)} \text{hasParWord}(W) \cdot \sum_{(p_1, p_2) \in W} |p_1 \cap p_2|$$

where

$$\text{hasParWord}(W) = \mathbb{I}[\text{wordMatches}(W) \geq 2]$$

$$\text{wordMatches}(W) = \sum_{(p_1, p_2) \in W} \mathbb{I}[|p_1 \cap p_2| > 0]$$

MBAWO calculates an internal maximally-weighted bipartite matching for token overlap; however, it only values those matches which correspond to parallel structure in the reference data. It enforces that through the function wordMatches.

Finally, we define the *maximum word overlap* (MWO) metric. MWO is at the opposite extreme of EPM; it does not necessarily control for the presence of parallel structure. Even so, its ability to measure a model's capacity to find *any* parallel words may be useful. Its functions are as follows:

$$\texttt{size}(p) = |\text{words}(p)|$$

$$\texttt{score}(p_1, p_2) = |\text{words}(p_1) \cap \text{words}(p_2)|$$

C Inter-Annotator Agreement Study

To provide some measure of the quality of our data, we performed an inter-annotator agreement study on the ASP dataset. Due to constraints on time and expertise, we recruited our third author, an experienced classicist and Latin teacher, to revisit eight sermons using our annotation scheme. To address the limited annotated data, we computed a bootstrapped estimate for agreement across the whole dataset. After obtaining an initial computation of inter-annotator agreement, we ran 1,000 trials to obtain a 95% confidence interval for our agreement scores. The number of items sampled was equivalent to the total number of matchings made in the initial computation.

Because the space of possible spans and links between spans is prohibitively large, we could not use more traditional inter-annotator agreement metrics such as Cohen's κ (Cohen, 1960) or Krippendorff's α (Krippendorff, 2019). Instead, we used our own metrics as defined in Section 5 and Appendix B. However, following the conclusions of Hripcsak and Rothschild that the F_1 measure converges to κ as the number of negative pairs grows increasingly large, we can treat our F_1 scores in a similar manner to chance-corrected agreement statistics.

As a final preprocessing step before matching annotations, we corrected them with two strategies to reduce noise. We felt that these strategies were warranted after discussion unearthed two vague points in our guidelines. We first describe our issues with the guidelines below, and then we clarify the annotation cleaning done afterward.

1. **Conjunctions**: It was unclear whether conjunctions meaningfully contributed to a parallelism. For some parallelisms, they may have been syntactically necessary—but did that mean that they should be part of the parallelism? We decided that conjunctions should be included if *every* branch of the parallelism has one; otherwise, they should be omitted. This allows polysyndeton to be recognized while avoiding the requisite but incidental connections created by some syntactic structure.

2. **Interlocking Parallelisms**: Second, it was difficult to determine the best way to partition parallel structure into branches. This was especially the case with longer parallelisms that involved multiple clauses. Take Fig. 7 as an example. Without clear rules, there are multiple ways to produce parallel structure:

   - Interpretation 1 considers each clause its own branch.
   - Interpretation 2 considers each pair of clauses, which juxtapose *inanis* ("without, lacking, empty") and *plenus* ("filled, full"), as a single parallelism; moreover, it also recognizes the similar syntactic relationships in the individual clauses.

Scoring Object	Actual F_1	Sample Mean and Deviation	Confidence Interval
Parallelism	0.4615	0.4124 ± 0.0303	$[0.4088, 0.4160]$
Branch	0.5084	0.5080 ± 0.0310	$[0.5043, 0.5117]$
Branched Words	0.5906	0.5973 ± 0.0322	$[0.5935, 0.6012]$
Words	0.6136	0.6130 ± 0.0312	$[0.6092, 0.6167]$

Table 6: Aggregated actual and sample inter-annotator agreement scores. All values are rounded to the fourth decimal place and range between 0 and 1. Higher is better for the actual F_1 and the sample mean; lower is better for the standard deviation. Smaller confidence intervals indicate greater stability of our estimate.

Latin	*inanis auro,*	*plenus deo*;	*inanis omni transitoria facultate,*	*plenus sui domini uoluntate.*
English	[he who] lacks gold,	[is] full of God;	[he who] lacks every transient supply,	[is] full of the Lord's own favor.
Interpretation 1				
Stratum 1	$P_{1,1}$	$P_{1,2}$	$P_{1,3}$	$P_{1,4}$
Stratum 2	–	–	–	–
Interpretation 2				
Stratum 1	$P_{1,1}$		$P_{1,2}$	
Stratum 2	$P_{2,1}$	$P_{2,2}$	$P_{3,1}$	$P_{3,2}$
Interpretation 3				
Stratum 1	$P_{1,1}$		$P_{1,2}$	
Stratum 2	–	–	–	–

Figure 7: Selection of possible interpretations of parallel structure of a passage from Augustine's *Sermones* (Sermon 177, Section 4). Clauses are aligned for the Latin and English at the top of the table. Each subsequent section of the table relays an interpretation of parallel structure; each $P_{i,j}$ indicates branch j of parallelism i.

- Interpretation 3 only annotates the first stratum of the prior interpretation.

Ultimately, we ruled that the third interpretation was best. It *maximally* captured the parallel structure in these clauses. Although it is true that each pair of clauses has its own relationships (*e.g.*, same number of words, same syntactic structure), these relationships also contribute to the larger structure they are contained within, as each *inanis* and *plenus* takes a noun of the same case (ablative) as its object. Thus, these connections are still captured in the third interpretation. We only advise differing from a maximal interpretation if the parallelisms intentionally use different features.

To address these issues in our original annotations, we automatically altered the annotations on two bases. First, if *all* branches of a parallelism were preceded by a conjunction, then conjunctions were included in all branches; otherwise, no conjunctions were permitted, and any present were removed from annotations. Second, we collapsed interlocking parallelisms into larger branches if they were adjacent. If these larger branches were part of

a nested parallelism, and such branches produced a parallelism on an earlier stratum, we removed these larger branches entirely. Although these alterations did cause gains in annotation agreement, they were all between roughly 0.02 to 0.03 F_1.

We present our inter-annotator agreement results in Table 6. Across the board, these scores fall below traditional standards (*i.e.*, above 0.67 at the very least) for good chance-corrected reliability in content analysis (Carletta, 1996). However, as noted by Artstein and Poesio, acceptable inter-annotator agreement values remain disputed; the earlier work by Landis and Koch denotes the range between 0.4 and 0.6 as *moderate* agreement and the range between 0.6 and 0.8 as *substantial* agreement.

Regardless of the exact standard that we follow, we do believe that the disagreement displayed by this inter-annotator agreement study is meaningful and in part due to some vagueness in our original guidelines. We have already updated our guidelines to provide greater specifications for future annotators, and we are currently working on improving our data with these guidelines. We hope to release an enhanced version of our dataset in future work.

D   Model Idiosyncrasies

In Section 6.2, we go over our general Encoder-CRF model architecture, and we describe some of the major components of our models. Due to space considerations, some details were omitted from that discussion. We discuss such details here.

D.1   Training `<UNK>` in BiLSTM-CRFs

In Encoder-CRF models which apply a word-level vocabulary, one necessary issue concerns the handling of unknown words. Usually, such models maintain an `<UNK>` token for such cases. However, if the `<UNK>` token is not seen during training, the model will not know how to use it and may confuse it with other tokens seen during training.

Various strategies have been employed to address this problem. Some decide that all words seen less than k times, where k is some preset value, become `<UNK>` tokens (Reimers and Gurevych, 2017). Others select singletons—words which only appear *once* in the training data—and alter them to become `<UNK>` during training with a predetermined fixed probability (Lample et al., 2016). We follow the latter strategy, but we augment it so that we can adapt the probability to the dataset at hand and can avoid choosing an arbitrary value.

We propose a singleton replacement probability analogous to Kneser-Ney smoothing (Ney et al., 1994). We compute the frequency of each type in the dataset. Then, we tally the number of types which occur exactly once, n_1, and the number of types which occur exactly twice, n_2. Here, we use notation from previous work where n represents the number of word types and the subscripts represent a conditional frequency on that count (Chen and Goodman, 1998). Finally, for the singleton replacement probability p_r, we use the equation:

$$p_r = \frac{n_1}{n_1 + 2n_2} \tag{1}$$

The Kneser-Ney replacement probability for the ASP dataset, given the current data splits, is approximately 0.6529.

D.2   Transformer Modifications

We apply the Transformer encoder in some of our models with a slight change from the usual implementation. In line with previous work which sees minor improvements in model performance (Chen et al., 2018; Wang et al., 2019; Nguyen and Salazar, 2019), we swap the traditional order of layer normalization and skip connections. Applying the notation of Nguyen and Salazar, we use `PreNorm` in the incorporation of the residual connection:

$$\mathbf{x}_{l+1} = \mathsf{LayerNorm}(\mathbf{x}_l + F_l(\mathbf{x}_l))$$

where l is the layer's index, F represents the layer itself, and `LayerNorm` represents the layer normalization operation (Ba et al., 2016).

D.3   Subword Blending

As previously mentioned, we use WordPiece tokenization with our models which either have a Transformer encoder or Latin BERT embeddings. Using subword-level tokens presents an issue for a word-level tagging problem: in what way should the model process subwords to generate word-level tags? The original BERT paper, which tackles NER, does not use a CRF and instead lets the tag classification of each word's first subword represent the whole word (Devlin et al., 2019).

We take inspiration from BERT's methods and others' approaches to handling subword-to-word relationships (Souza et al., 2019; Casas et al., 2020) by putting a *blending* layer into the architecture. As mentioned in Section 6.2, the blending layer's objective is to combine subword-level encodings into word-level encodings. We define three variations:

- **Take-First**: In this approach, we mimic BERT and select the first subword of each word as its representative. (Note that, when convenient, we abbreviate this variant as "tf".)

- **Mean**: In this approach, we take the mean of all subword encodings per word. This is akin to a subword-aware mean pooling layer.

- **Sum**: In this approach, we sum all subword encodings for a word to represent it. This representation may allow for a model to recognize the accumulation of multiple subwords.

E   Data Splitting Approach

As noted in Section 4, parallelisms are not evenly distributed over sections. Sections are also not evenly distributed over documents. Because we performed evaluation in terms of documents, we wanted to apply a simple heuristic to guarantee that the data splits would fairly distribute tags.

To do this, we used a straightforward approach to optimize split creation. To apply the approach, we supplied it with a set of ratios which govern the quantity and relative size of the splits. We began by taking each file in the dataset and computing

Dataset	Split	Optimal Ratio	Inner Tag Ratio	Outer Tag Ratio
ASP	Training	0.7	0.7021	0.7020
	Validation	0.1	0.0982	0.1008
	Optimization	0.1	0.0946	0.0980
	Test	0.1	0.1051	0.0992
PSE-I	Training	0.7	0.6947	0.7007
	Validation	0.1	0.1026	0.0998
	Optimization	0.1	0.1005	0.0997
	Test	0.1	0.1022	0.0998

Table 7: Data split ratio results. All ratios are rounded to the fourth decimal place.

Dataset	Compared Splits		Inner p-Value	Inner Statistic	Outer p-Value	Outer Statistic
ASP	Training	Validation	0.5797	0.5722	0.6284	0.4990
	Training	Optimization	0.8347	−0.2162	0.7557	−0.3236
	Training	Test	0.7210	0.3668	0.4727	0.7405
	Validation	Optimization	0.5705	−0.5816	0.5631	−0.5942
	Validation	Test	0.8557	−0.1848	0.9601	0.0509
	Optimization	Test	0.6751	0.4290	0.4980	0.7038
PSE-I	Training	Validation	0.7476	−0.3236	0.6212	−0.4972
	Training	Optimization	0.9533	−0.0588	0.8240	0.2235
	Training	Test	0.9882	−0.0148	0.2588	1.1381
	Validation	Optimization	0.8291	0.2166	0.5779	0.5588
	Validation	Test	0.7987	0.2560	0.2526	1.1540
	Optimization	Test	0.9720	0.0353	0.5651	0.5780

Table 8: Data split Welch's t-Test results. All p-values and statistics are rounded to the fourth decimal place.

Dataset	Split	Parallelisms	Branches	Branched Tokens	Tokens
ASP	Training	1448	3264	13833	94740
	Validation	208	478	1935	13580
	Optimization	191	424	1863	13196
	Test	215	485	2070	13440
	Total	2062	4651	19701	134956
PSE-I	Training	541	1478	17736	168848
	Validation	87	236	2618	24152
	Optimization	77	219	2565	24064
	Test	81	220	2610	24139
	Total	786	2153	25529	241203

Table 9: Data split results per relevant object count. Note that "branched tokens" refers to all tokens in branches—not the number of tokens in general.

counts of its *outer* and *inner* tags.[11] A tag is an outer tag if it is O or M; otherwise, it is an inner tag. Then, we attempted to place a file in each split. If placing that file in a split minimized the mean-squared error (MSE) among the splits, then the file was placed in that split. To be specific, we averaged the MSE for inner and outer tags to compute the final MSE. We repeated this process for every file.

As a further heuristic, we sorted the files after their inner and outer tag counts were computed. We did so by the number of inner tags from maximum to minimum, breaking ties by the number of outer tags. This was in line with our objective to balance out the parallelisms and branches seen across splits: the ordering allowed for files which have a greater effect on MSE to be placed first, thereby letting files with less tags smooth out error gradually.

To verify our procedure, we provide the resulting mean-squared error for our splits. We also used Welch's t-test for this purpose. For each pair of splits created, we ran this test twice with per-file counts of the inner and outer tags. In this case, we do *not* want the test to report significance; rather, in showing that the difference between the distri-

---

[11]As in the main paper, we created *strata* of tags for each dataset equal to the maximum nesting depth of a branch.

butions is insignificant (*e.g.*, $p \geq 0.05$), we are showing that the splits are divided up such that they could have been drawn from the same distribution. We use the SciPy implementation of Welch's *t*-test for this purpose (Virtanen et al., 2020).

F Hyperparameter Search Spaces

For our hyperparameter search experiments in Section 7.2, we performed a random hyperparameter search (Bergstra and Bengio, 2012) of eight trials per setting. However, because we are proposing a new task, we did not have prior literature on successful hyperparameters which we could draw upon in order to define hyperparameter spaces. Thus, to perform these experiments, we created our own.

These hyperparameter search experiments were governed by three main elements:

1. The set of hyperparameters which are selected for variation. Although many hyperparameters could be varied, only some were chosen to direct the search toward hyperparameters which were suspected to be meaningful.

2. The space itself from which hyperparameters were drawn, as this determines all possible values which the hyperparameter can take.

3. The set of constraints which are imposed upon the random trials. Naturally, we want to prevent any trial from being duplicated; however, there are other inductive biases which may guide our search.

In the subsections below, we expound upon each of these elements and provide tables which summarize pertinent information regarding them.

F.1 Selected Hyperparameters

Table 11 provides information about what hyperparameters are varied per model. Due to space considerations, we use a number of abbreviations; these are supplied in Table 10.

F.2 Designated Hyperparameter Spaces

Table 12 lists the hyperparameter spaces which we used during the random search process. While some of the above hyperparameters are relatively self-explanatory in their functionality, we provide an explanation for those which may be less clear or otherwise warrant further explanation:

- Activation Function: The PyTorch (Paszke et al., 2019) implementation of the Transformer (Vaswani et al., 2017) provides integrations for both ReLU and GeLU (Hendrycks and Gimpel, 2016) as activation functions. We uphold that support in our modifications (as presented in Appendix D.2) to see whether they have any major effects on our results.

- Dimensionalities: For all embedding and hidden dimensionality spaces, we let the search space be in powers of two and at every value averaged between adjacent powers of two. We used this approach to explore a decent portion of the search space without leaving big gaps between larger powers. Furthermore, we differed the spaces for BiLSTMs and Transformers to adapt more to precedent while still allowing some exploration. In particular, we took inspiration from some hyperparameter LSTM searches in NER (Reimers and Gurevych, 2017) and the general application of the Transformer (Vaswani et al., 2017).

- Depth: In initial trials, we found that high depth values prevented the models from learning meaningful information. Thus, instead of setting a maximum of 6 encoder layers as per the initial Transformer implementation (Vaswani et al., 2017), we lowered it to 4.

- Learning Rates: In the NER literature, a variety of learning rates have been used (alongside a variety of optimizers). Values from .1 (Huang et al., 2015) to .015 (Ma and Hovy, 2016) to .01 (Lample et al., 2016) to a variety of manually-tuned others (Reimers and Gurevych, 2017) have been proposed. Due to the differences in our task, however, we examine a wider range on the basis of those values. Previous experience in using Adam (Kingma and Ba, 2015) has seen models struggle with high learning rates, hence the choice of varying between lower ones.

For all such hyperparameter search spaces, we sampled from each uniformly.

F.3 Hyperparameter Trial Constraints

Although we could theoretically generate any combination of hyperparameters in our randomly-sought trials, it is not necessarily the case that any combination will be fruitful. With a wide enough search space, it is possible that random search will

Abbreviation	Full Hyperparameter Name
AF	Activation Function
BF	Blending Function
HS	Hidden Size
IS	Input Size
LR	Learning Rate
Lemma	Lemmatization

Table 10: List of all hyperparameter abbreviations.

Embedding	Encoder	Varied Hyperparameters
Learned (Word)	BiLSTM	Depth, HS, IS, LR, Lemma
word2vec	BiLSTM	Depth, HS, LR
Learned (Subword)	Transformer	AF, BF, Depth, Heads, HS, IS, LR
(Chinese/Latin) BERT	–	BF, LR
(Chinese/Latin) BERT	BiLSTM	BF, Depth, HS, LR
(Chinese/Latin) BERT	Transformer	AF, BF, Depth, Heads, HS, LR

Table 11: Listing of all hyperparameters varied per model.

Hyperparameter	Space
Activation Function	{ReLU, GeLU}
Blender	{mean, sum, take-first}
Depth	{1, 2, 3, 4}
Heads	{1, 2, 4, 8}
Hidden Size (BiLSTM)	{32, 48, 64, 96, 128, 192, 256, 384, 512}
Hidden Size (Transformer)	{256, 384, 512, 768, 1024, 1280, 1536, 1792, 2048}
Input Size (BiLSTM)	{64, 96, 128, 192, 256, 384, 512, 768}
Input Size (Transformer)	{128, 192, 256, 384, 512, 768, 1024}
Learning Rate	{0.0001, 0.0002, . . . , 0.01}
Lemmatization	{True, False}

Table 12: Collection of all hyperparameter search spaces.

avoid discovering regions of the search space where performance is approximately maximal. As a result, we direct the random search process in some cases by forcing trials to meet a set of constraints.

The main constraint we supplied was for the BiLSTM-based models. This constraint was the *word-level dimensionality compression* constraint, which assured that HS $\leq$ IS. The hidden state is intended here to compress and learn how to use word embedding information. This constraint is applied implicitly for the model with BERT embeddings and the BiLSTM encoder, as every dimensionality in the search space was at or below 768.

G   Error Analysis

The main body of this paper, and especially Section 7.2, highlights major hyperparameters for our Encoder-CRF architecture which improve performance. In this section, we attempt to provide some insight about where our Encoder-CRF models could still improve by describing the kinds of errors that these models make. We focus on the ASP dataset in this section, as this dataset was designed for word-level parallelism detection.

To elucidate relevant and constructive model behavior, we defined a set of categories for this error analysis. That set of categories can be divided into a three-by-three grid on the basis of three error *granularities* and three error *types*. Following our

	Parallelism		Branch			Word			Total
	FP	FN	FP	FN	FM	FP	FN	FM	(by Sermon)
Sermon 24	8	22	3	3	2	0	2	0	40
Sermon 175	7	13	0	3	0	1	1	0	25
Sermon 177	11	39	2	2	1	0	1	0	56
Sermon 188	7	7	2	0	0	0	4	0	20
Sermon 207	7	4	2	0	0	1	0	0	14
Sermon 211	4	19	0	1	0	0	1	0	25
Sermon 219	0	9	0	0	0	0	0	0	9
Sermon 222	1	1	0	0	0	0	0	0	2
Sermon 271	0	5	0	0	0	0	0	0	5
Total (by Category)	45	119	9	9	3	2	9	0	196

Table 13: A presentation of our error analysis categorization results on ASP's validation set with the model with the highest F_1 score from Section 7.2.

metrics, these granularities are at the levels of parallelisms, branches, and words. Meanwhile, two of our error types derive from classification error types: *false positive* (FP) and *false negative* (FN).

Our third error type, *false mixture* (FM), is a combination of the FP and FN which applies to branches and words. Because a model can both predict a branch or word that a parallelism does not contain (false positive) and omit a branch or word that a parallelism contains (false negative), both error types are simultaneously possible for these granularities. Conversely, a parallelism cannot both be entirely missing and entirely distinct from reference data; thus, the granularity-type combination of parallelism and false mixture is not possible. This leaves us with a set of eight categories.

We went over ASP's validation set with this annotation scheme, comparing hypothesized parallelisms from the model with the highest-scoring F_1 score from Section 7.2 and reference parallelisms. We added a category for every matched hypothesis parallelism and reference parallelism. In other words, a hypothesis and reference are only categorized once if they have some overlap; otherwise, they are categorized independently. We provide a more detailed, category-by-category overview of this scheme in our main code repository.

We present the results of our error analysis categorization in Table 13. From this table, we see that the predominant cause of error comes from the highest level of granularity: parallelisms. Conversely, we see that other kinds of error are quite infrequent. As a result, we can surmise that these Encoder-CRF models are relatively all-or-nothing

in their sequence labeling approach. They are proficient at getting entire parallelisms correct, and largely down to the boundaries, when they detect a parallelism. However, their ability to confidently detect them in full needs more work.

To illustrate some of these error categories, we provide a set of three examples in Fig. 8. Fig. 8(a) presents the most common case: the false negative parallelism. Fig. 8(b), in turn, presents its false positive version. Finally, Fig. 8(c) shows what a false mixture looks like.

Starting with Fig. 8(a), we find a two-branch parallelism from ASP. Both branches contain two clauses spanning four words, are headed by subjects of the same case and number, and apply verbal forms in their first clauses with the same lemma (*promitto*). Augustine plays up contrasts by juxtaposing human beings and God as well as verbs for belief (*crederes*) and doubt (*dubitas*). The moods used to define the conditional structures of each branch, being contrafactual and factual, respectively, further highlight this contrast. In short, these clauses contain many distinct cues as to their parallel nature. In spite of this, our model did not detect this pair. One possibility is that variations on token order due to function words (*si*, *et*) and commas caused the model to ignore the branch pair.

Next, Fig. 8(b) shows a predicted parallelism that the reference data did not contain. On the one hand, there are aspects of this branch pair that make them seem parallel. The clauses juxtapose heaven (*caeli*, *de caelo*) and earth (*terreno*, *terrae*) in the same grammatical roles. Both also use verbs conjugated in the same manner, and each takes a direct object

(a) [*homo*   *si promitteret*   , *crederes*   ]$_1$; [*deus*
     human:NOM;SG if promise:IPFV;ACT;SBJV;3SG , believe:IPFV;ACT;SBJV;2SG ; god:NOM;SG

     promittit   , *et dubitas*   ]$_1$?
     promise:PRS;ACT;IND;3SG , and doubt:PRS;ACT;IND;2SG ?

     "If a human were promising, you would believe them; God promises, and you doubt Him?"

(b) *... quam illa quae* ⟨ *caeli*   *creatorem de caelo deposuit*   ⟩$_1$, *et* ⟨
     ... than that who heaven:GEN;SG maker:ACC;SG from sky:ABL;SG put.down:PRF;ACT;IND;3SG , and

     terreno corpore terrae induit   *conditorem*   ⟩$_1$; *...*
     earthen:ABL;SG body:ABL;SG earth:GEN;SG clothe:PRF;ACT;IND;3SG builder:ACC;SG ; ...

     "... than that which put the maker of heaven down from heaven, and that which clothed the builder of the earth with an earthen body; ..."

(c) *fecit enim hoc* [⟨ *per*   *fideles suos*   ]$_1$, [⟨ *per christianos suos*   ⟩$_1$]$_1$, ⟨ *per*
     do for this through faithful:ACC;PL own:ACC;PL , through christian:ACC;PL own:ACC;PL , through

     potestates   ⟩$_1$ *a se ordinatas et christi iugo iam subditas* .
     authority:ACC;PL by oneself govern and christ yoke already subject .

     "For he did this through his own faithful, through his own Christians, through the authorities governed by him and subjected already to the yoke of Christ."

Figure 8: Examples of errors for the ASP dataset's validation set and the model with the highest F_1 score from Section 7.2. Blue square brackets demarcate branches in the reference data, red triangular brackets demarcate branches in the hypothesis data, and numbering indicates the parallelism to which a branch belongs relative to its data source. Below each Latin sentence, we provide a word-by-word English translation, gloss some morphological features in branches, and present an idiomatic translation. Example (a) is from Sermon 177, Section 11 and displays a parallelism-level false negative. Example (b) is from Sermon 207, Section 1 and displays a parallelism-level false positive. Example (c) is from Sermon 24, Section 7 and displays a branch-level false mixture.

in the same case (*creatorem*, *conditorem*) which are synonymous. On the other hand, the word order in these clauses calls their parallel nature into question; there is no clear alignment between the word orders in each clause (*e.g.*, the direct objects are the second and fifth words, respectively). As a result, it seems understandable both why the model was fooled by this sentence as well as why it was not annotated in the first place.

Finally, we provide an example of a branch-level false mixture in Fig. 8(c). In this branch-level false mixture, the model agrees with the reference parallelism on its second branch. However, it both ignores the reference's first branch and adds an additional branch after the second. The reference contains a relatively simple parallelism consisting of two three-word branches centering around two prepositional phrases that share the word *suos*. The pair are followed by a third clause that is not part of the parallelism due to its rather elaborate content and lack of *suos* (although, it contains the related form *se*). To speculate about the model's mistake, it may have been drawn by lexical connections between the second branch and the final clause (*i.e.*, *per* with *per*, *suos* with *se*, and *christianos* with *christi*). However, because of the final clause's additional complexity, it then only selected a couple words to pair with the second branch.

H Exhaustive Experimental Results

In this section, we display box plots which give an overview of all F_1 scores attained from each of the best models across all configurations explored during the hyperparameter search and all metrics. All box plots are created from 16 data points, as each model architecture variation (*i.e.*, embedding-encoder combination) was examined across sixteen distinct tagging schemes. The ASP dataset's plots are presented in Figs. 9 to 12. Meanwhile, the PSE-I dataset's plots are presented in Figs. 13 to 16. We also provide tabular data and CSV data for all our results, additionally including precision and recall for all metrics, in our main code repository.

I Exemplary Model Hyperparameter Tables

In this section, we provide sets of tables which describe the hyperparameters used for each best trial catalogued in Appendix H. For the ASP dataset, we organized the results into three tables—Tables 14 to 16—based upon what hyperparameters were varied. For the PSE-I dataset, we organized them similarly in Tables 17 and 18.
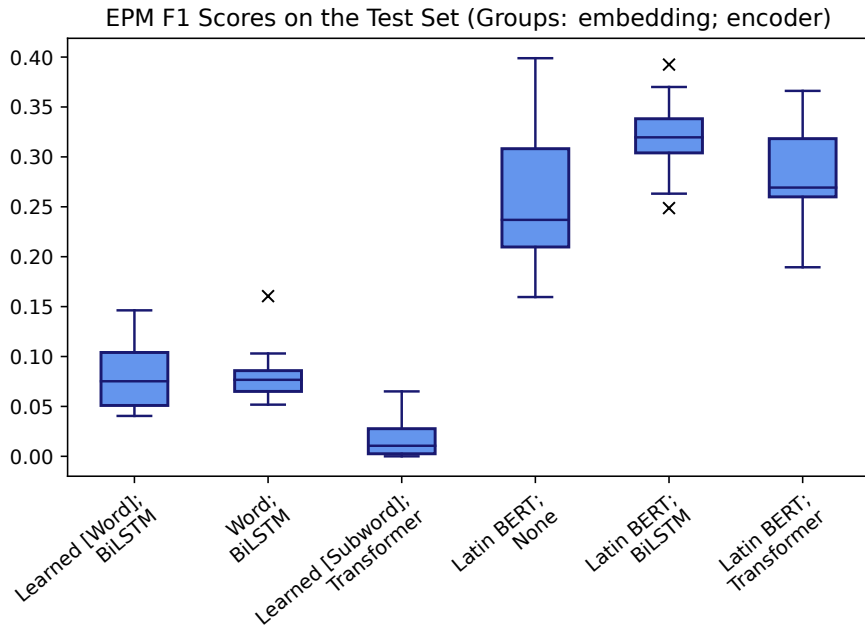
Figure 9: Box plots presenting model-relative results on the ASP dataset's test set using the Exact Parallelism Match (EPM) metric.

Figure 10: Box plots presenting model-relative results on the ASP dataset's test set using the Maximum Parallel Branch Match (MPBM) metric.

Figure 11: Box plots presenting model-relative results on the ASP dataset's test set using the Maximum Branch-Aware Word Overlap (MBAWO) metric.

Figure 12: Box plots presenting model-relative results on the ASP dataset's test set using the Maximum Word Overlap (MWO) metric.
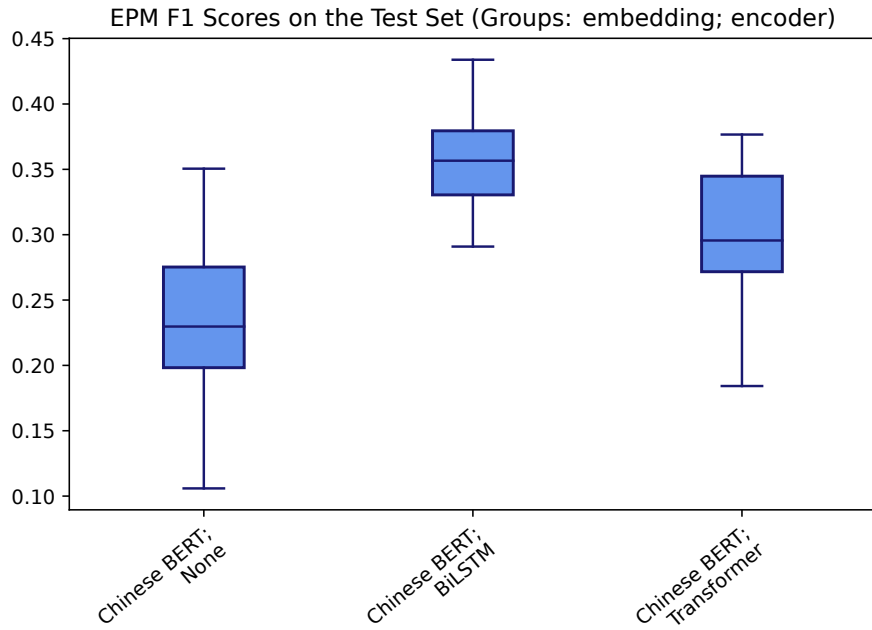
Figure 13: Box plots presenting model-relative results on the PSE-I dataset's test set using the Exact Parallelism Match (EPM) metric.
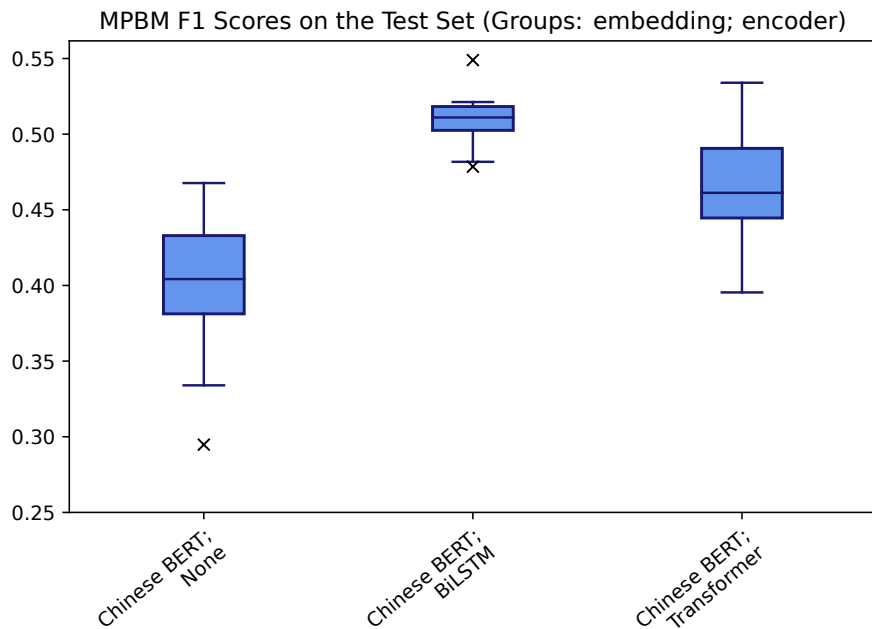
Figure 14: Box plots presenting model-relative results on the PSE-I dataset's test set using the Maximum Parallel Branch Match (MPBM) metric.
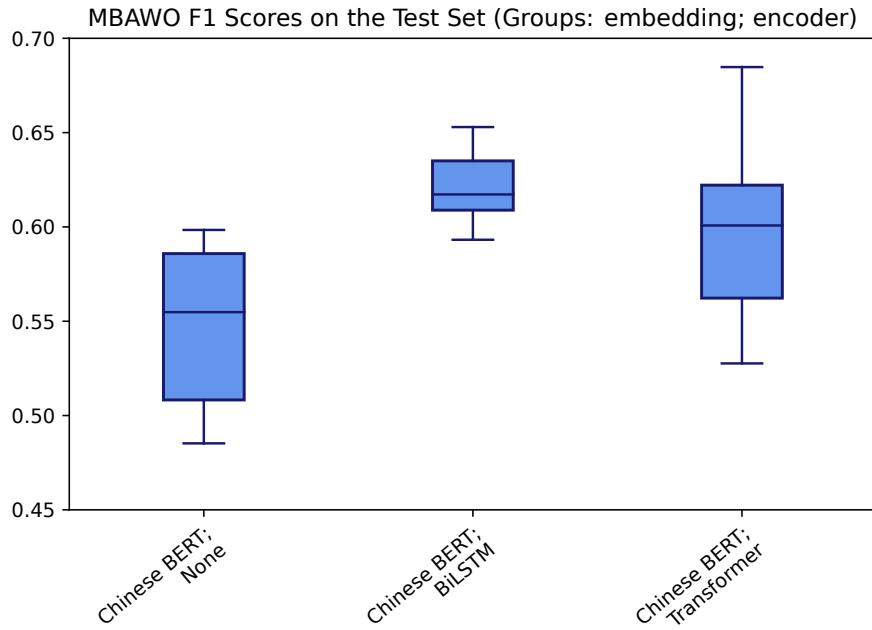
Figure 15: Box plots presenting model-relative results on the PSE-I dataset's test set using the Maximum Branch-Aware Word Overlap (MBAWO) metric.
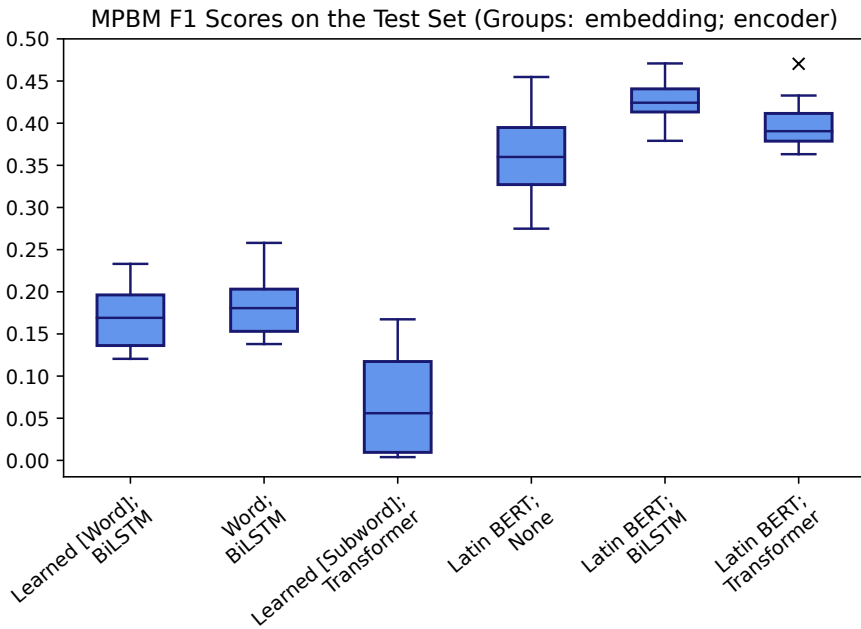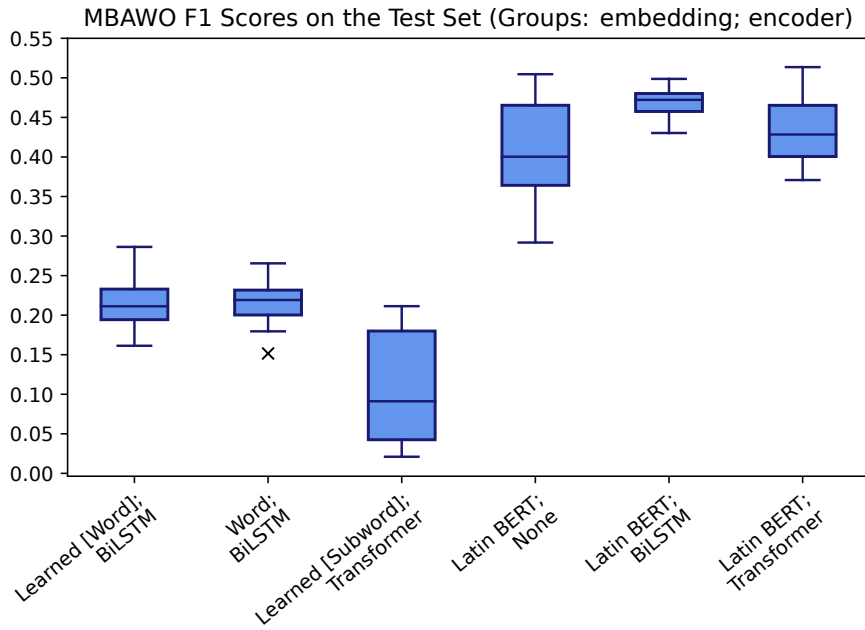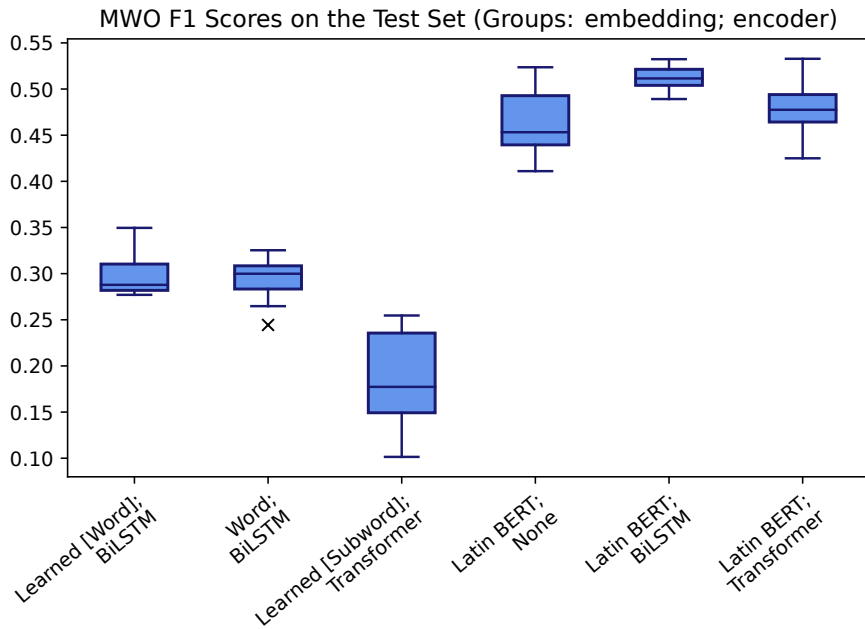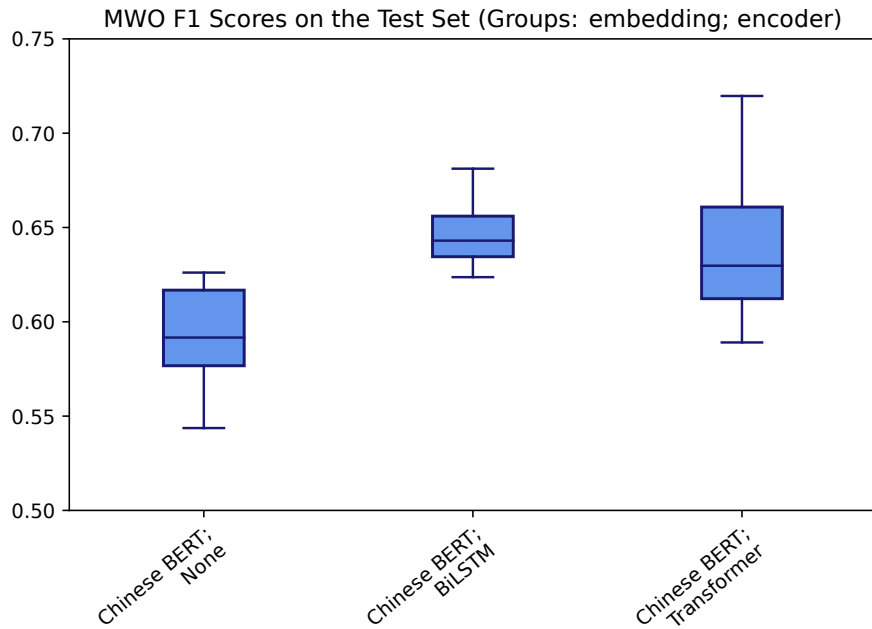

Figure 16: Box plots presenting model-relative results on the PSE-I dataset's test set using the Maximum Word Overlap (MWO) metric.

Model Components		Tagging Scheme		Hyperparameters				
Embedding	Encoder	Tagset	Link Type	DEPTH	HS	IS	LEMMA	LR
Learned (Word)	BiLSTM	BIO	Token	3	384	512	N	0.0013
			Branch	4	384	768	N	0.0008
		BIOE	Token	4	64	768	N	0.0021
			Branch	3	48	256	N	0.0039
		BIOJ	Token	1	64	512	N	0.0076
			Branch	3	384	384	N	0.0028
		BIOM	Token	4	128	384	N	0.0010
			Branch	1	128	128	N	0.0035
		BIOJE	Token	4	256	768	N	0.0063
			Branch	2	256	256	Y	0.0034
		BIOME	Token	4	32	192	N	0.0045
			Branch	4	128	256	N	0.0082
		BIOMJ	Token	4	96	512	N	0.0052
			Branch	2	64	768	N	0.0047
		BIOMJE	Token	3	192	512	Y	0.0018
			Branch	3	128	192	Y	0.0085
word2vec	BiLSTM	BIO	Token	4	96	300	Y	0.0028
			Branch	3	256	300	Y	0.0040
		BIOE	Token	3	32	300	Y	0.0076
			Branch	3	128	300	Y	0.0029
		BIOJ	Token	3	48	300	Y	0.0072
			Branch	4	64	300	Y	0.0059
		BIOM	Token	3	256	300	Y	0.0028
			Branch	4	256	300	Y	0.0059
		BIOJE	Token	3	32	300	Y	0.0035
			Branch	4	48	300	Y	0.0049
		BIOME	Token	4	192	300	Y	0.0002
			Branch	3	32	300	Y	0.0032
		BIOMJ	Token	1	256	300	Y	0.0035
			Branch	4	96	300	Y	0.0058
		BIOMJE	Token	3	128	300	Y	0.0022
			Branch	4	192	300	Y	0.0028

Table 14: Best hyperparameters for non-BERT models with a BiLSTM encoder for the ASP dataset.

Model Components		Tagging Scheme		Hyperparameters						
Embedding	Encoder	Tagset	Link Type	AF	BF	Depth	Heads	HS	IS	LR
Learned (Subword)	Transformer	BIO	Token	ReLU	sum	3	4	384	192	0.0081
			Branch	ReLU	mean	1	4	768	128	0.0076
		BIOE	Token	ReLU	tf	1	1	1280	192	0.0071
			Branch	GeLU	tf	2	8	384	768	0.0095
		BIOJ	Token	GeLU	tf	2	4	512	1024	0.0052
			Branch	GeLU	mean	1	8	2048	768	0.0043
		BIOM	Token	ReLU	tf	2	8	1792	192	0.0011
			Branch	GeLU	mean	1	4	2048	256	0.0060
		BIOJE	Token	GeLU	sum	2	2	512	768	0.0082
			Branch	ReLU	mean	2	1	384	128	0.0051
		BIOME	Token	GeLU	sum	4	8	1280	384	0.0071
			Branch	GeLU	sum	2	8	384	384	0.0056
		BIOMJ	Token	ReLU	sum	3	2	512	384	0.0065
			Branch	GeLU	tf	2	2	384	512	0.0100
		BIOMJE	Token	ReLU	mean	4	4	256	192	0.0087
			Branch	GeLU	sum	3	8	1280	512	0.0100
Latin BERT	Transformer	BIO	Token	GeLU	sum	1	8	256	768	0.0090
			Branch	ReLU	mean	4	1	1024	768	0.0086
		BIOE	Token	ReLU	sum	4	4	1280	768	0.0028
			Branch	ReLU	sum	3	2	768	768	0.0034
		BIOJ	Token	ReLU	mean	4	1	1792	768	0.0007
			Branch	GeLU	mean	4	1	1024	768	0.0021
		BIOM	Token	GeLU	sum	3	2	1024	768	0.0035
			Branch	GeLU	sum	3	2	1024	768	0.0035
		BIOJE	Token	GeLU	mean	2	1	1792	768	0.0048
			Branch	GeLU	mean	2	4	1536	768	0.0037
		BIOME	Token	GeLU	mean	4	4	1024	768	0.0016
			Branch	GeLU	sum	2	2	1536	768	0.0033
		BIOMJ	Token	ReLU	tf	3	1	384	768	0.0061
			Branch	ReLU	mean	2	1	1536	768	0.0014
		BIOMJE	Token	ReLU	mean	4	1	256	768	0.0086
			Branch	GeLU	mean	3	8	384	768	0.0045

Table 15: Best hyperparameters for models with a Transformer encoder on the ASP dataset.

Model Components		Tagging Scheme		Hyperparameters			
Embedding	Encoder	Tagset	Link Type	BF	DEPTH	HS	LR
Latin BERT	–	BIO	Token	sum	–	–	0.0055
			Branch	tf	–	–	0.0010
		BIOE	Token	sum	–	–	0.0012
			Branch	sum	–	–	0.0055
		BIOJ	Token	tf	–	–	0.0077
			Branch	sum	–	–	0.0070
		BIOM	Token	tf	–	–	0.0064
			Branch	sum	–	–	0.0012
		BIOJE	Token	sum	–	–	0.0063
			Branch	mean	–	–	0.0005
		BIOME	Token	mean	–	–	0.0045
			Branch	mean	–	–	0.0021
		BIOMJ	Token	tf	–	–	0.0005
			Branch	mean	–	–	0.0030
		BIOMJE	Token	sum	–	–	0.0001
			Branch	mean	–	–	0.0061
Latin BERT	BiLSTM	BIO	Token	mean	3	384	0.0007
			Branch	sum	3	96	0.0022
		BIOE	Token	tf	4	48	0.0024
			Branch	mean	3	512	0.0012
		BIOJ	Token	mean	3	256	0.0008
			Branch	sum	4	128	0.0066
		BIOM	Token	sum	2	192	0.0048
			Branch	tf	3	192	0.0073
		BIOJE	Token	mean	4	48	0.0017
			Branch	sum	3	128	0.0010
		BIOME	Token	mean	2	64	0.0083
			Branch	sum	4	128	0.0026
		BIOMJ	Token	sum	3	96	0.0028
			Branch	tf	4	192	0.0013
		BIOMJE	Token	sum	4	192	0.0055
			Branch	mean	2	96	0.0086

Table 16: Best hyperparameters for models with BERT-based embeddings and a non-Transformer encoder on the ASP dataset.

Model Components		Tagging Scheme				Hyperparameters					
Embedding	Encoder	Tagset	Link Type	AF	BF	Depth	Heads	HS	IS	LR
Chinese BERT	Transformer	BIO	Token	ReLU	sum	2	8	1280	768	0.0010
			Branch	ReLU	sum	2	2	1792	768	0.0040
		BIOE	Token	ReLU	tf	1	1	256	768	0.0088
			Branch	GeLU	tf	2	2	1280	768	0.0010
		BIOJ	Token	ReLU	tf	4	8	1536	768	0.0063
			Branch	ReLU	tf	1	1	512	768	0.0078
		BIOM	Token	GeLU	tf	4	1	256	768	0.0100
			Branch	ReLU	mean	1	8	1792	768	0.0094
		BIOJE	Token	GeLU	tf	2	4	1536	768	0.0016
			Branch	ReLU	sum	1	2	1536	768	0.0061
		BIOME	Token	GeLU	mean	2	4	2048	768	0.0001
			Branch	GeLU	mean	1	8	1536	768	0.0086
		BIOMJ	Token	GeLU	mean	2	4	768	768	0.0025
			Branch	ReLU	mean	3	2	1280	768	0.0076
		BIOMJE	Token	ReLU	mean	3	4	512	768	0.0073
			Branch	GeLU	sum	3	4	384	768	0.0020

Table 17: Best hyperparameters for models with a Transformer encoder on the PSE-I dataset.

Model Components		Tagging Scheme		Hyperparameters			
Embedding	Encoder	Tagset	Link Type	BF	DEPTH	HS	LR
Chinese BERT	–	BIO	Token	tf	–	–	.0002
			Branch	mean	–	–	.0089
		BIOE	Token	mean	–	–	.0063
			Branch	mean	–	–	.0012
		BIOJ	Token	mean	–	–	.0043
			Branch	sum	–	–	.0072
		BIOM	Token	sum	–	–	.0020
			Branch	mean	–	–	.0006
		BIOJE	Token	mean	–	–	.0050
			Branch	tf	–	–	.0028
		BIOME	Token	mean	–	–	.0087
			Branch	tf	–	–	.0037
		BIOMJ	Token	mean	–	–	.0092
			Branch	tf	–	–	.0017
		BIOMJE	Token	tf	–	–	.0052
			Branch	mean	–	–	.0066
Chinese BERT	BiLSTM	BIO	Token	mean	4	192	.0012
			Branch	sum	2	96	.0019
		BIOE	Token	sum	3	32	.0025
			Branch	sum	2	64	.0043
		BIOJ	Token	sum	2	512	.0002
			Branch	mean	1	48	.0007
		BIOM	Token	mean	3	128	.0080
			Branch	mean	2	32	.0056
		BIOJE	Token	mean	4	64	.0040
			Branch	sum	4	128	.0003
		BIOME	Token	tf	4	32	.0016
			Branch	tf	4	32	.0010
		BIOMJ	Token	sum	3	128	.0004
			Branch	sum	4	48	.0011
		BIOMJE	Token	tf	1	32	.0058
			Branch	mean	2	32	.0025

Table 18: Best hyperparameters for models with BERT-based embeddings and a non-Transformer encoder on the PSE-I dataset.